1, 3 and 4) and Q2417X, previously reported in the Singaporean Chinese population, in one family (family 2) of the four Taiwanese IV families studied here (Fig. 1).

Sequencing of the entire coding region of *FLG* revealed a previously unidentified *FLG* mutation, E1795X, in the proband, her father and paternal grandmother of family 1 (Fig. 1). Presence of the mutation E1795X was confirmed by enzyme digestion assay using restriction enzyme BfaI (Fig. 1). This mutation was not detected in 50 unrelated control alleles. The proband in family 1 was compound heterozygous for E1795X and 3321delA and showed a much more severe phenotype than that of her parents, consistent with the reported semidominant pattern of inheritance.[2]

Discussion

Previously reported *FLG* mutations seem to be population specific. Several prevalent *FLG* mutations were reported in the European populations.[4] However, these mutations were rarely found in the Japanese[6] or in the Singaporean Chinese populations.[8] The Japanese and the Singaporean Chinese populations were reported to have *FLG* mutations specific to their own populations (Fig. 2).[6–8] In a single case, the European-specific mutation R501X was identified in a Japanese family;[10] however, haplotype analysis showed that the mutation was not inherited from a European ancestor but recurred *de novo* in Japan.

Until now, no *FLG* mutations have been described in the Taiwanese population. In the present study, we identified three *FLG* mutations in the Taiwanese population. Interestingly, one *FLG* mutation 3321delA is prevalent in the Japanese population.[6,9] Another mutation Q2417X was found in the Singaporean Chinese population.[8] The remaining mutation, E1795X, is a previously unidentified *FLG* mutation which might be unique in the Taiwanese population. The Taiwanese are a mixture of people originating from both south and north China, and native Taiwanese people. The Japanese population comprises native Japanese and immigrants from the Asian

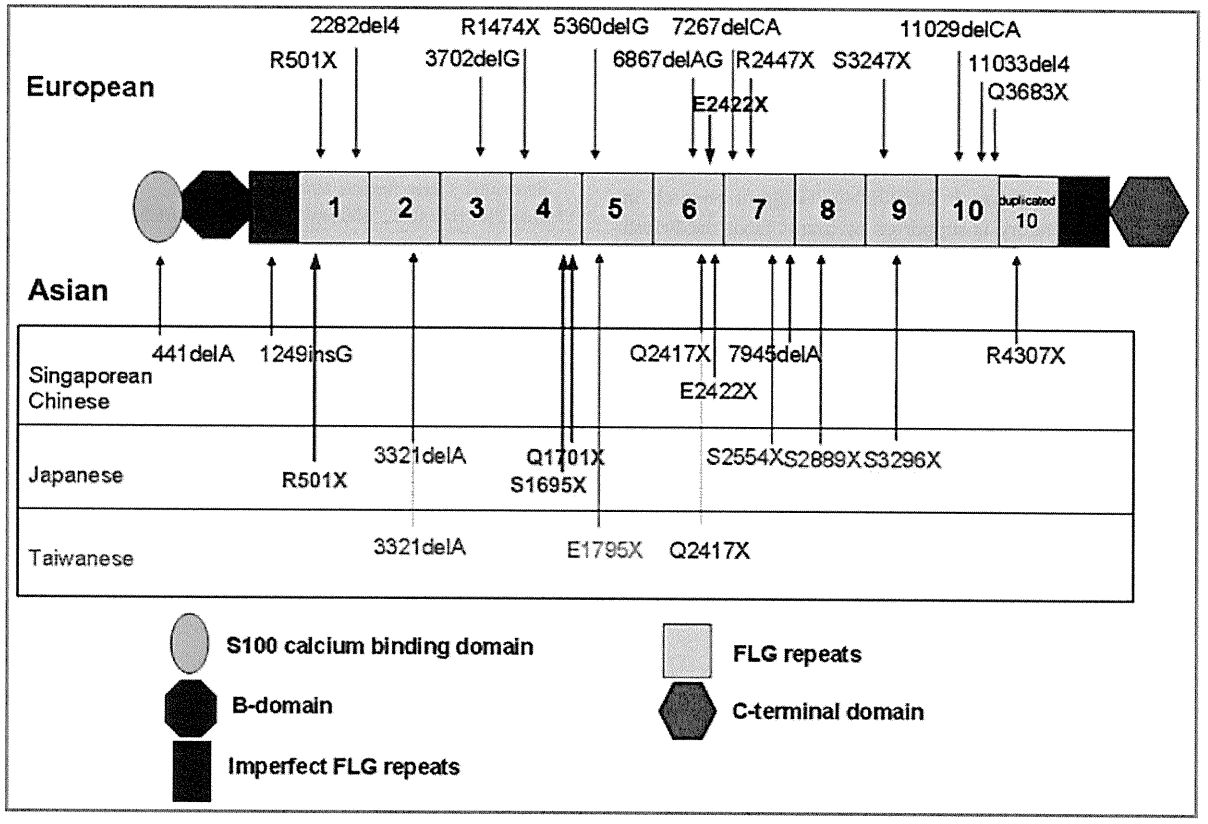

Fig 2. Difference in *FLG* mutations between European and Asian populations. Molecular structure of profilaggrin and *FLG* mutations detected among the European (top) and the Asian (bottom) populations. Profilaggrin contains 10–12 highly homologous filaggrin-repeat domains. *FLG* mutations among the European and the Asian populations appear to be unique. The previously identified *FLG* mutation 3321delA in the Japanese population (red) and Q2417X in the Singaporean Chinese population (blue) are found in the present Taiwanese IV families. E1795X is a previously unidentified mutation. Interestingly, the Taiwanese population shares *FLG* mutations with both the Singaporean Chinese population (Q2417X) and the Japanese population (3321delA), although the Singaporean Chinese population and the Japanese population do not share any of the known *FLG* mutations.

continent via Korea or China. Thus, the present results might be reasonable from the aspect of East Asian population genetics.

None of the previously reported *FLG* mutations identified in the European population was found in the Taiwanese population. The present results further support the notion that *FLG* mutation spectra of the white European and the Asian ancestral groups are different, as 25–50% of patients with atopic eczema are expected to harbour *FLG* mutations.[4,6] In such patients, skin barrier defects due to filaggrin deficiency are thought to play an essential role in the pathogenesis of the disease.[11,12] Thus, it is very important and useful for us to know whether a patient with atopic eczema has an *FLG* mutation or not, when we see the patient. However, every population is likely to have a unique set of *FLG* mutations. Specifically, we cannot use the prevalent European FLG mutations to screen Asian patients with atopic eczema. For the proper population-specific mutation screening, we have to obtain information on prevalent *FLG* mutations in each population. It is therefore important to clarify the worldwide population genetics of *FLG* mutations.

Acknowledgments

We thank the patients for their generous cooperation and Ms Akari Nagasaki for her fine technical assistance on this project. We thank Dr James R. McMillan for proofreading of this manuscript. This work was supported in part by Grants-in-Aid from the Ministry of Education, Science, Sports, and Culture of Japan to M.A. (Kiban B 20390304). Filaggrin research in the McLean laboratory is supported by grants from the British Skin Foundation, the National Eczema Society, the Medical Research Council (reference number G0700314) and donations from anonymous families affected by eczema in the Tayside Region of Scotland.

References

1 Sybert VP, Dale BA, Holbrook KA. Ichthyosis vulgaris: identification of a defect in synthesis of filaggrin correlated with an absence of keratohyaline granules. *J Invest Dermatol* 1985; **84**:191–4.
2 Smith FJ, Irvine AD, Terron-Kwiatkowski A *et al.* Loss-of-function mutations in the gene encoding filaggrin cause ichthyosis vulgaris. *Nat Genet* 2006; **38**:337–42.
3 Akiyama M, Shimizu H. An update on molecular aspects of the non-syndromic ichthyoses. *Exp Dermatol* 2008; **17**:373–82.
4 Sandilands A, Terron-Kwiatkowski A, Hull PR *et al.* Comprehensive analysis of the gene encoding filaggrin uncovers prevalent and rare mutations in ichthyosis vulgaris and atopic eczema. *Nat Genet* 2007; **39**:650–4.
5 O'Regan GM, Sandilands A, McLean WHI, Irvine AD. Filaggrin in atopic dermatitis. *J Allergy Clin Immunol* 2008; **122**:689–93.
6 Nomura T, Akiyama M, Sandilands A *et al.* Specific filaggrin mutations cause ichthyosis vulgaris and are significantly associated with atopic dermatitis in Japan. *J Invest Dermatol* 2008; **128**:1436–41.
7 Nomura T, Akiyama M, Sandilands A *et al.* Prevalent and rare mutations in the gene encoding filaggrin in Japanese patients with ichthyosis vulgaris and atopic dermatitis. *J Invest Dermatol* 2008; DOI 10.1038/jid.2008.372.
8 Chen H, Ho JC, Sandilands A *et al.* Unique and recurrent mutations in the filaggrin gene in Singaporean Chinese patients with ichthyosis vulgaris. *J Invest Dermatol* 2008; **128**:1669–75.
9 Nomura T, Sandilands A, Akiyama M *et al.* Unique mutations in the filaggrin gene in Japanese patients with ichthyosis vulgaris and atopic dermatitis. *J Allergy Clin Immunol* 2007; **119**:434–40.
10 Hamada T, Sandilands A, Fukuda S *et al.* *De novo* occurrence of the filaggrin mutation p.R501X with prevalent mutation c.3321delA in a Japanese family with ichthyosis vulgaris complicated by atopic dermatitis. *J Invest Dermatol* 2008; **128**:1323–5.
11 Elias PM, Hatano Y, Williams ML. Basis for the barrier abnormality in atopic dermatitis: outside-inside-outside pathogenic mechanisms. *J Allergy Clin Immunol* 2008; **121**:1337–43.
12 Nemoto-Hasebe I, Akiyama M, Nomura T *et al.* Clinical severity correlates with impaired barrier in filaggrin-related eczema. *J Invest Dermatol* 2009; **129**:682–9.

Carcinogenesis vol.30 no.9 pp.1597–1605, 2009
doi:10.1093/carcin/bgp160
Advance Access publication July 7, 2009

Deficient deletion of apoptotic cells by macrophage migration inhibitory factor (MIF) overexpression accelerates photocarcinogenesis

Ayumi Honda[1,2,†], Riichiro Abe[2,†], Yoko Yoshihisa[1], Teruhiko Makino[1], Kenji Matsunaga[1], Jun Nishihira[3], Hiroshi Shimizu[2] and Tadamichi Shimizu[1,*]

[1]Department of Dermatology, Graduate School of Medicine and Pharmaceutical Sciences, University of Toyama, Sugitani, Toyama 930-0194, Japan, [2]Department of Dermatology, Hokkaido University Graduate School of Medicine, Sapporo 060-8638, Japan and [3]Department of Medical Information, Hokkaido Information University, Ebetsu 069-8585, Japan

*To whom correspondence should be addressed. Tel: +81 76 434 7305; Fax: +81 76 434 5028;
Email: shimizut@med.u-toyama.ac.jp

Chronic ultraviolet (UV) exposure can increase the occurrence of p53 mutations, thus leading to a dysregulation of apoptosis and the initiation of skin cancer. Therefore, it is extremely important that apoptosis is induced quickly after UV irradiation, without any dysregulation. Recent studies have suggested a potentially broader role for macrophage migration inhibitory factor (MIF) in growth regulation via its ability to antagonize p53-mediated gene activation and apoptosis. To further elucidate the possible role of MIF in photocarcinogenesis, the acute and chronic UVB effect in the skin was examined using macrophage migration inhibitory factor transgenic (MIF Tg) and wild-type (WT) mice. The MIF Tg mice exposed to chronic UVB irradiation began to develop skin tumors after ~14 weeks, whereas the WT mice began to develop tumors after 18 weeks. A higher incidence of tumors was observed in the MIF Tg in comparison with the WT mice after chronic UVB irradiation. Next, we clarified whether the acceleration of photo-induced carcinogenesis in the MIF Tg mice was mediated by the inhibition of apoptosis There were fewer sunburned cells in the epidermis of the MIF Tg mice than the WT mice after acute UVB exposure. The epidermis derived from the MIF Tg mice exhibited substantially decreased levels of p53, bax and p21 after UVB exposure in comparison with the WT mice. Collectively, these findings suggest that chronic UVB exposure enhances MIF production, which may inhibit the p53-dependent apoptotic processes and thereby induce photocarcinogenesis in the skin.

Introduction

Exposure to ultraviolet (UV) radiation leads to various acute deleterious cutaneous effects including sunburn and immunosuppression and also long-term consequences such as premature aging and the potential development of skin cancers (1). UV radiation, particularly UVB, which has a wavelength of between 280 and 320 nm, has been suggested epidemiologically and has been demonstrated experimentally to be the pivotal causal factor for skin cancer in humans and other animals (2). Chronic UVB-induced inflammation and directly damaged DNA can be correlated with skin tumor formation (3,4). Furthermore, the inability to adequately repair DNA after UVB irradiation can result in the formation of skin cancers (5). Chronic UV exposure can increase p53 mutations, thus leading to a dysregulation of apoptosis, an expansion of mutated keratinocytes and the initiation of skin cancer (6).

Abbreviations: CPD, cyclobutane pyrimidine dimmer; IL, interleukin; MIF, macrophage migration inhibitory factor; MIF Tg, macrophage migration inhibitory factor transgenic; mRNA, messenger RNA; PBS, phosphate-buffered saline; TUNEL, terminal deoxynucleotidyl transferase nick end labeling; TNF, tumor necrosis factor; UV, ultraviolet; WT, wild-type.

[†]These authors contributed equally to this work.

There is emerging evidence that keratinocytes participate in cutaneous inflammatory reactions and immune responses by producing a variety of cytokines. UV irradiation may trigger cutaneous inflammatory responses by stimulating epidermal keratinocytes to produce biologically potent cytokines such as interleukin (IL)-1 (7,8), IL-6 (9) and tumor necrosis factor (TNF)-α (10). These cytokines are involved not only in the mediation of local inflammatory reactions but also play discrete roles in tumor promotion (11).

The cytokine macrophage migration inhibitory factor (MIF) was first discovered 40 years ago as a T-cell-derived factor that inhibited the random migration of macrophages (12,13). Recently, MIF was reevaluated as a proinflammatory cytokine and pituitary-derived hormone that potentiates endotoxemia (14). Subsequent work has showed that T cells and macrophages secrete MIF in response to glucocorticoids as well as upon activation by various proinflammatory stimuli (15). It has been reported that MIF is expressed primarily in T cells and macrophages; however, recent studies have revealed this protein to be ubiquitously expressed in various cells (16–20). Skin melanoma cells express MIF messenger RNA (mRNA) and produce MIF protein (21). The expression of MIF mRNA and the production of MIF protein have been shown to be much higher in human melanoma cells than in cultured normal melanocytes. Therefore, MIF functions as a novel growth factor that stimulates uncontrolled growth and invasion of tumor cells (16,21,22). In addition, recent studies have suggested a potentially broader role for MIF in growth regulation because of its ability to antagonize p53-mediated gene activation and apoptosis (23,24).

In the skin, keratinocytes are capable of producing a variety of cytokines and are thought to be a principal source of cytokines from the epidermis after UV irradiation. Previous studies have shown enhanced MIF production in the skin after UVB irradiation (25,26). Solar UV light is a combination of both UVB and UVA wavelengths, each of which stimulate MIF production in both keratinocytes and fibroblasts in the skin. To further elucidate the possible role of MIF in UV-induced carcinogenesis and cell apoptosis, the acute and chronic effect of UVB in skin carcinogenesis was examined using macrophage migration inhibitory factor transgenic (MIF Tg) mice.

Materials and methods

Materials

The following materials were obtained from commercial sources. The Isogen RNA extraction kit was obtained from Nippon Gene (Tokyo, Japan); the DNA random primer labeling kit from Takara (Kyoto, Japan); [^{32}P]dCTP from DuPont-NEN (Boston, MA); anti-CPDs polyclonal antibody from Cosmo Bio Co, Ltd (Tokyo, Japan); anti-p53 polyclonal antibody from Novocastra Lab (Newcastle, UK); anti-p21 polyclonal antibody and anti-BAX polyclonal antibody from Santa Cruz Biotechnology (Santa Cruz, CA) and anti-β-actin antibodies purchased from Sigma–Aldrich Co (St Louis, MO); the western blot detection system was obtained from Cell Signaling Technology (Beverly, MA). The anti-MIF polyclonal antibody was prepared as described previously (27). The Cell Death Detection Kit was provided from Roche Molecular Biochemicals (Indianapolis, IN). Other reagents were of analytical grade.

Mice

The MIF-overexpressed transgenic mice were established following cDNA microinjection and the physical and biochemical characteristics, including body weight, blood pressure, serum levels of cholesterol and blood sugar, were normal as reported previously (28). The expression of the transgene was regulated by a hybrid promoter composed of the cytomegalovirus enhancer and β-actin/β-globin promoter, as reported previously (29). Strain of original MIF-Tg is ICR and backcrossed with C57BL/6 for at least 10 generations. Tg mice were maintained by heterozygous sibling mating. Transgenic and wild-type (WT) mice were maintained under specific-pathogen-free conditions at the Institute for Animal Experiments of Hokkaido University School of Medicine. Experiments using mice were conducted according to the guidelines set out by

the Hokkaido University Institutional Animal Care and Use Committee under an approved protocol. All experiments were performed on 8-week-old male adult mice.

UVB irradiation

UVB light source was a FL20SE30 (Clinical Supply Co, Tokyo, Japan) fluorescent lamp that emits 1.0 mW/cm^2 of UV between 280 and 370 nm (peak 305 nm) at a distance of 25 cm, as measured by UV radiometer (Torex Co, Tokyo, Japan). In short-term UVB experiments, MIF Tg and WT mice had their backs shaved with electric clippers and exposed to 200 mJ/cm^2 UVB. After UVB irradiation, the mice were euthanized at the indicated time points. Skin sections were excised from the dorsal surface and used for western blot analyses or immunohistochemical staining. In some experiments for UVB-induced cutaneous inflammation, UVB radiation was administered three times weekly (on days 1, 3 and 5) and skin was obtained on day 7. To examine UVB-induced carcinogenesis, MIF Tg and WT mice had their backs shaved with electric clippers once a week and were UVB irradiated in separate compartments of a modified mouse cage. An incrementally graded UV protocol was used (30): three times weekly a UV dose was delivered of 2.25 kJ/m^2 for 12 treatments (weeks 1–4), 4.05 kJ/m^2 for 24 treatments (weeks 5–12), 5.1 kJ/m^2 for 12 treatments (weeks 13–16) and 6 kJ/m^2 for 33 treatments (week 17 to the end of the experiment at the 27th week).

Skin tumors

Mice were monitored for tumor formation each week. The time to tumor development was taken as the time up to the appearance of a palpable swelling >1 mm subsequently diagnosed as a tumor on histopathological examination after 27 weeks. The tumor size was estimated after 27 weeks using orthogonal linear measurements made with Vernier calipers according to the following formula: volume (mm^3) = [(width, mm)^2 × (length, mm)]/2. The tumors were excised and preserved in 10% formalin, sectioned, stained with hematoxylin and eosin and examined microscopically. The groups each contained 12 MIF Tg and 12 WT mice.

Northern blot analysis

Total cellular RNA was isolated from the epidermis using an Isogen extraction kit according to the manufacturer's protocol. The epidermis was separated from the dermis by incubation in 0.5% dispase in RPMI 1640 at 37°C for 1 h. RNA was quantified by spectrophotometry and equal amounts of RNA (10 μg) from each sample were loaded on a formaldehyde–agarose gel. The gel was stained with ethidium bromide to visualize the RNA standards and the RNA was transferred onto a nylon membrane. Fragments obtained by restriction enzyme treatment for MIF and glyceraldehyde-3-phosphate dehydrogenase were labeled with [α-^{32}P]dCTP using a DNA random primer labeling kit. Hybridization was carried out using the mouse MIF cDNA probe as previously described (28). The membrane was washed twice with 2× saline and sodium citrate (16.7 mM NaCl, 16.7 mM sodium citrate) at 22°C for 5 min, twice with 0.2× saline and sodium citrate containing 0.1% sodium dodecyl sulfate at 65°C for 15 min and twice with 2× saline and sodium citrate at 22°C for 20 min prior to autoradiography. A quantitative densitometric analysis was performed using an MCID Image Analyzer (Fuji Film, Tokyo, Japan). The density of MIF bands was normalized by the intensities of glyceraldehyde-3-phosphate dehydrogenase.

Western blot analysis

The epidermis of each mouse was homogenized with a Polytron homogenizer (Kinematica, Lausanne, Switzerland). The protein concentrations of the cell homogenates were quantified using a Micro BCA protein assay reagent kit. Equal amounts of homogenates were dissolved in a 20 μl solution contained of Tris–HCl, 50 mM (pH 6.8), containing 2-mercaptoethanol (1%), sodium dodecyl sulfate (2%), glycerol (20%) and bromophenol blue (0.04%) and the samples were heated to 100°C for 5 min. The samples were then subjected to sodium dodecyl sulfate–polyacrylamide gel electrophoresis and electrophoretically transferred onto a nitrocellulose membrane. The membranes were blocked with 1% non-fat dry milk powder in phosphate-buffered saline (PBS), probed with antibodies against p53, bax and p21 and subsequently reacted with secondary IgG antibodies coupled with horseradish peroxidase. The resultant complexes were processed for the detection system according to the manufacturer's protocol. The relative amounts of proteins associated with specific antibodies were normalized according to the intensities of β-actin.

Immunohistochemical analysis

Five micrometers thick section of dorsal skin were fixed in 10% neutral buffered formalin. After deparaffinization, the sections were treated with target retrieval solution (DAKO, Carpinteria, CA), washed three times with PBS and incubated in H_2O_2/methanol/PBS solution (1:50:50) for 15 min to block endogenous peroxidase activity. After three washes in PBS with 0.5% Tween, the sections were preincubated for 10 min in 10% normal goat serum in PBS and then were incubated with the first antibody overnight at 4°C. After three washes in PBS plus 0.5% Tween, the sections were incubated for 1 h at room temperature with the secondary antibodies. After washing in PBS, staining was performed using the Vectastain Elite ABC kit with diaminobenzidine as the chromagen, according to the manufacturer's instructions (Vector Laboratories, Burlingame, CA). As a negative control, the tissue sections were stained with normal serum and the secondary antibody.

UVB-induced apoptosis in cultured keratinocytes of MF Tg and WT. Mouse keratinocyte (second passage) from MIF Tg or C57BL/6 mice were irradiated with UVB at 50 mJ/cm^2. After 24 h, irradiated cells were analyzed for terminal deoxynucleotidyl transferase nick end labeling (TUNEL) assay or western blot for p53.

TUNEL assay. Cells undergoing apoptosis were detected using TUNEL according to the manufacturer's recommended procedure (R&D Systems, Minneapolis, MN). For statistical analysis, apoptotic cells were counted by light microscopy (×100) and expressed as the mean number (±SD) of apoptotic cells per section. Five random fields per section (one section per mouse, five mice per group) were analyzed.

Cultured apoptotic cells were also detected using TUNEL. Incorporated fluorescein was detected by anti-fluorescein monoclonal antibody Fab fragments from sheep, conjugated with alkaline phosphatase.

Statistics

Values are expressed as the mean ± SEM of the respective test or control group. Statistical significance between the control group and test groups was evaluated by either the Student's *t*-test or one-way analysis of variance.

Results

Enhanced expression of MIF in MIF Tg mice epidermis

MIF expression in the MIF Tg mouse epidermis was first examined after UVB irradiation. Northern blot analysis revealed that 16 h after 200 mJ/cm^2 UVB irradiation, MIF Tg mice showed higher levels of MIF mRNA expression even before irradiation. After UVB exposure, the MIF mRNA expression dramatically increased in comparison with that of the WT mice (Figure 1).

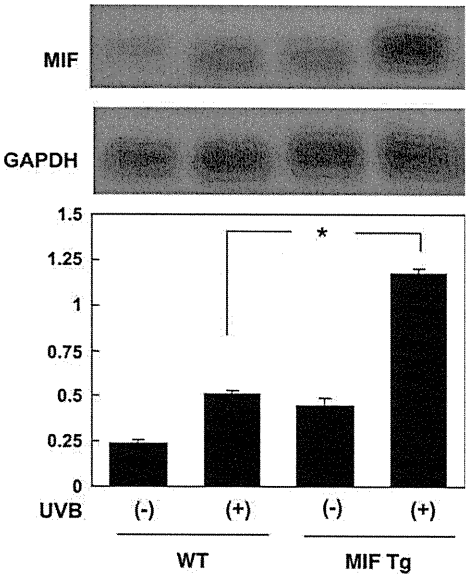

Fig. 1. Enhanced expression of MIF in the MIF Tg mouse epidermis after UV exposure. The expression of MIF mRNA was examined. Total RNA was isolated at 16 h after UVB (200 mJ/cm^2) and analyzed by northern blotting. MIF Tg mice (n = 5) showed higher levels of MIF mRNA expression even before irradiation. After UVB exposure, MIF mRNA expression dramatically increased in comparison with that of WT mice (n = 5). The experiments were repeated three times with similar results.

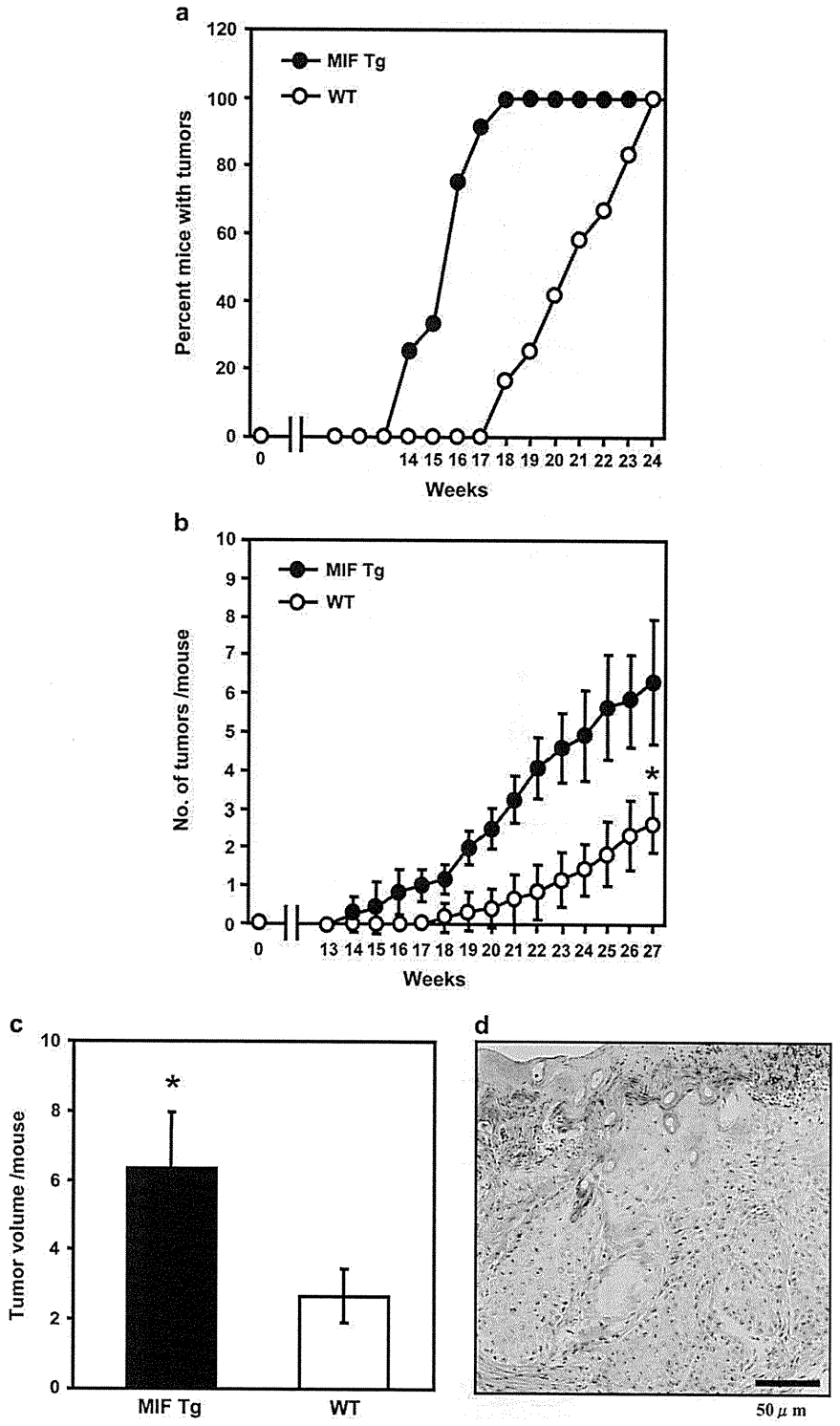

Fig. 2. Accelerated UVB-induced carcinogenesis in the MIF Tg mice. (**a**) MIF Tg and WT mice were subjected to chronic UVB. The details of the protocols are described in Materials and Methods. The formation of skin tumors was determined on a weekly basis. MIF Tg mice exposed to chronic UVB began to develop skin tumors after ~14 weeks, whereas the WT mice began to develop tumors after 18 weeks. (**b**) The incidence of skin tumors was recorded weekly and a tumor was considered to occur when an outgrowth of >1 mm in diameter was observed. MIF Tg mice developed a higher number of tumors in each mouse in comparison with WT mice ($^*P < 0.001$). (**c**) The mice were UVB irradiated as in (b). At the end of study at week 27, the volume of all tumors on each mouse was recorded ($^*P < 0.001$). (**d**) The histopathology of well-differentiated squamous cell carcinoma from an MIF Tg mouse. Scale bar indicates 100 μm (hematoxylin and eosin staining).

Sensitivity of MIF Tg mice to the development of skin tumors elicited by chronic exposure to UVB

To examine the role of MIF for chronic UV-induced carcinogenesis, MIF Tg and WT mice were subjected to chronic UVB as described in the Materials and Methods and followed up for the formation of skin tumors on a weekly basis. The MIF Tg mice exposed to chronic UVB began to develop skin tumors after ~14 weeks, whereas WT mice began to develop tumors after 18 weeks (Figure 2a). The mean time for tumor development in MIF Tg mice was after 110.3 ± 9.0 days, whereas it was 147.0 ± 15.5 days in WT mice. MIF Tg mice developed a higher number of tumors in each mouse in comparison with WT mice. At the 27th week, the average number of tumors per mouse was 6.33 ± 1.61 in the MIF Tg mice, whereas there were only 2.67 ± 0.78 in the WT mice ($P < 0.001$; Figure 2b). The volume of tumors developed in UVB-irradiated MIF Tg mice was significantly higher in comparison with that of WT mice ($P < 0.001$) (Figure 2c). Tumors measuring <2 mm in diameter proved to be too small for a reliable histological analysis and were assumed to be papillomas. Lesions that were ~2 mm in diameter had multilayered epithelia with irregular cells. These lesions were similar to actinic keratosis, and some large tumors (>3 mm in diameter) were diagnosed as well-differentiated SCC (Figure 2d). Twelve unirradiated MIF Tg mice and 12 unirradiated WT mice developed no tumors during the course of this study.

TUNEL-positive cells in UV-irradiated MIF Tg mouse epidermis

The possible role of MIF in UV-induced cell apoptosis was examined using MIF Tg and WT mice. Twenty-four hours after 200 mJ/cm^2 UVB irradiation, large numbers of sunburned cells and TUNEL-positive cells were detected in the WT mice, whereas, there were fewer sunburned cells and TUNEL-positive cells detected in MIF Tg mice (Figure 3a). Thereafter, the number of TUNEL-positive nuclei in the MIF Tg mice was compared with that in the WT mice. MIF Tg mice showed a significantly smaller number of apoptotic cells than the WT mice ($P < 0.01$; Figure 3b).

Immunohistochemistry: accumulation of DNA damages in the epidermis following UVB. We then investigated cyclobutane pyrimidine dimmers (CPD), as UV-induced DNA damage photoproduct

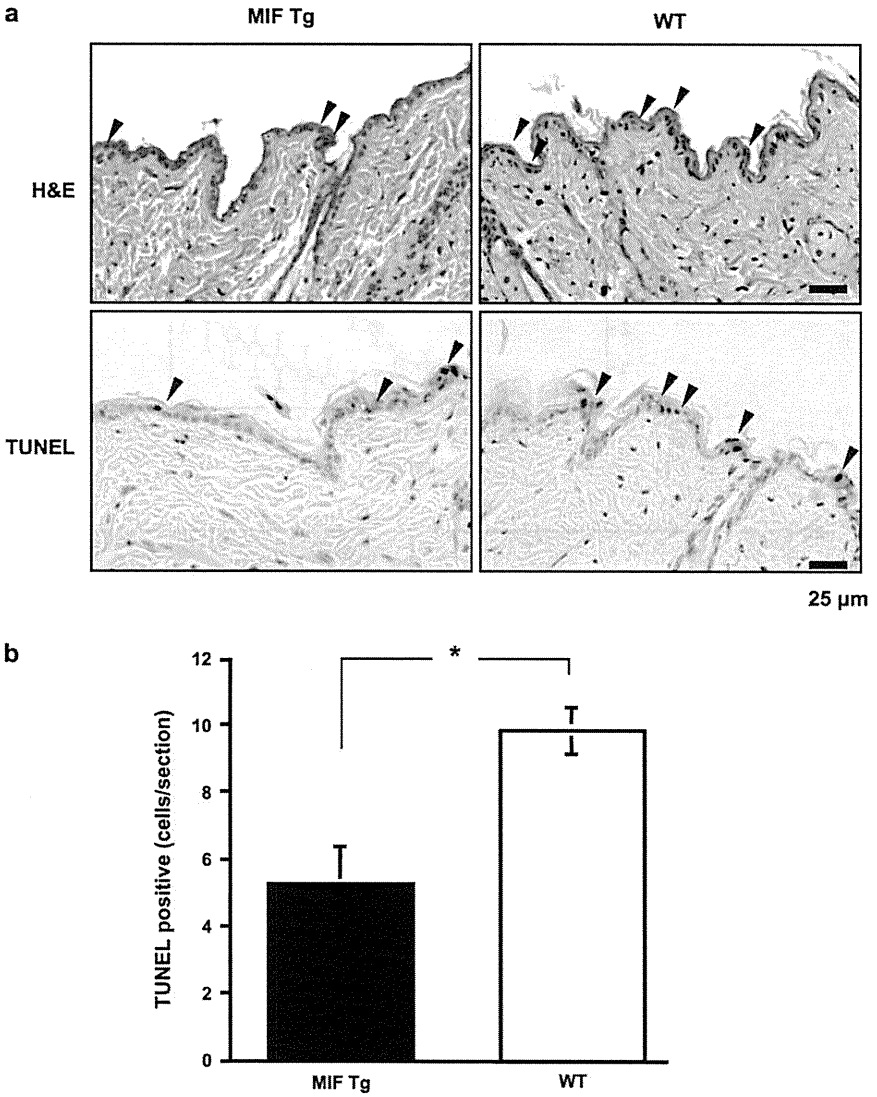

Fig. 3. Sunburn cells in UV-irradiated MIF Tg mouse epidermis. (**a**) Hematoxylin and eosin (H&E) staining and TUNEL assay for the detection of apoptotic cells in the epidermis of MIF Tg and WT mice skin 24 h after UVB irradiated (200 mJ/cm^2). Sunburn cells and TUNEL-positive cells are indicated by arrowheads. The scale bar indicates 25 μm. (**b**) The numbers of TUNEL-positive nuclei of MIF Tg mice were compared with the WT mice. Each value represents the mean ± SEM ($n = 5$). Smaller numbers of TUNEL-positive cells were observed in the MIF Tg in comparison with the WT mouse skin ($^*P < 0.01$).

(31) in UVB-irradiated skin. Twenty-four or 48 hours after 200 mJ/cm^2 UVB irradiation, a large number of CPD-positive cells was detected in MIF Tg mice. Whereas, there were fewer CPD-positive cells detected in WT mice (Figure 4a). Thereafter, the number of CPD-positive cell in the MIF Tg mice was significantly higher compared with that in the WT mice ($P < 0.001$; Figure 4b).

p53, bax and p21 expression in UV-irradiated MIF Tg mice epidermis

p53 is a key factor in the photoreactive process and bax and p21 are important downstream proteins regulated by p53. To further confirm the role of MIF in influencing p53-mediated gene activation, the time course for the induction of p53, bax and p21 in 200 mJ/cm^2 UVB-irradiated mouse epidermis was investigated by western blot analysis with specific antibodies. The epidermis derived from MIF Tg mice exhibited decreased induction levels of p53 at 12 and 24 h after irradiation in comparison with the WT mice (Figure 5a). Similarly, the induction levels of bax and p21 from the MIF Tg mice substantially decreased in comparison with those of the WT mice at 48 and 72 h after UVB exposure. An immunohistochemical analysis revealed that at 24 h after UVB irradiation, intense nuclear p53 immunostaining was observed in the WT mice epidermis. In contrast, nuclear p53 immunostaining was low in the MIF Tg mice (Figure 5b). Similarly, at 48 h after UVB irradiation, a low level of p21 expression in and around the nuclei was observed in the MIF Tg mice in comparison with the WT mice. Bax immunoreactivity was both perinuclear and cytoplasmic and the MIF Tg mice showed a lower expression level compared with that of the WT mice at 48 h (Figure 5b).

UVB-induced cutaneous inflammation in MIF Tg and WT mice

UVB-induced infiltration of leukocytes is a major source of inflammatory reactions. Therefore, the effect of UVB-induced infiltration was examined in MIF Tg and WT mice after three courses of UVB exposure. UVB exposure in the MIF Tg mice resulted in greater leukocyte infiltration than in the UVB-irradiated WT mice skin ($P < 0.05$; Figure 6).

UVB-induced apoptosis in cultured keratinocytes of MF Tg and WT mice

To confirm that MIF overexpression prevents keratinocyte apoptosis, cultured keratinocyte from the MIF Tg or the WT mice were irradiated with UVB at 50 mJ/cm^2. After 24 h, irradiated cells were analyzed for TUNEL assay or western blot for p53. As shown in Figure 7a and b, apoptotic keratinocytes (TUNEL positive) from MIF Tg mice were significantly reduced compared with that of WT mice ($P < 0.005$). Furthermore p53 expression of MIF Tg keratinocytes was also lower than that of WT mice (Figure 7c).

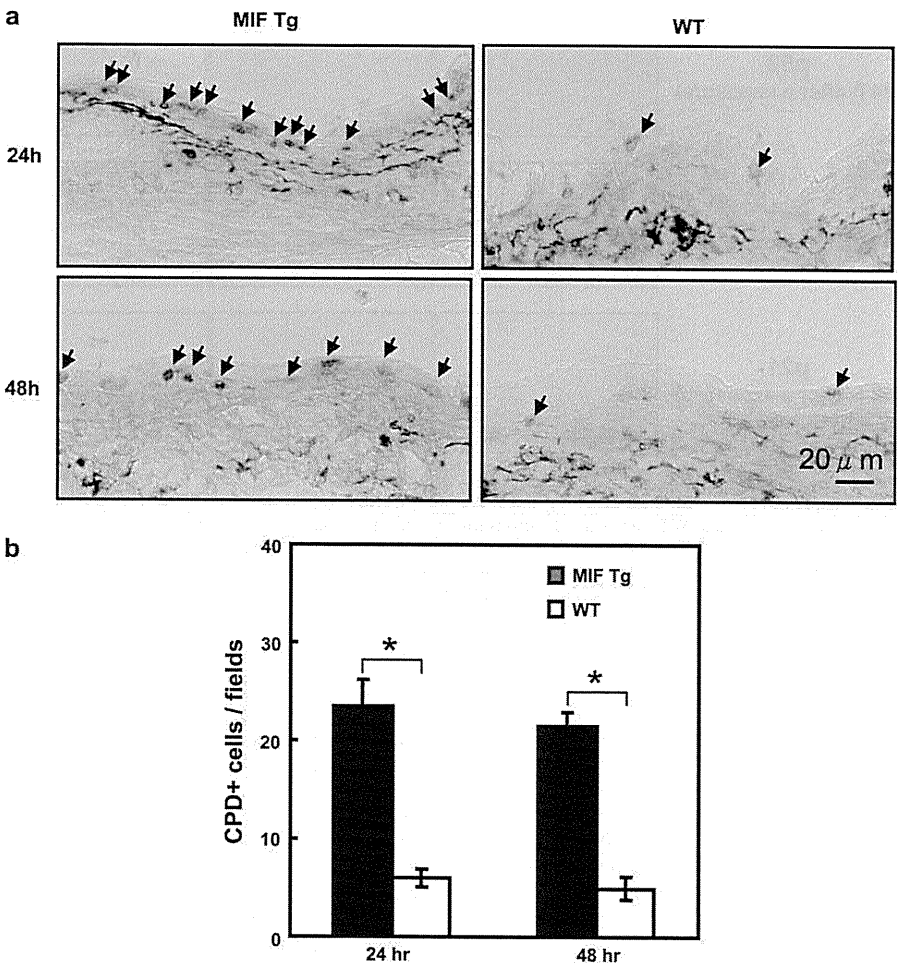

Fig. 4. CPD-positive cells in UV-irradiated MIF Tg mouse epidermis. (**a**) CPD staining in the epidermis of MIF Tg and WT mice skin 24 or 48 h after UVB irradiated (200 mJ/cm^2). CPD-positive cells indicated by arrowheads. Scale bar indicates 20 μm. (**b**) The numbers of CPD-positive cells of MIF Tg mice were compared with WT mice. Each value represents the mean ± SEM ($n = 5$) (*$P < 0.001$).

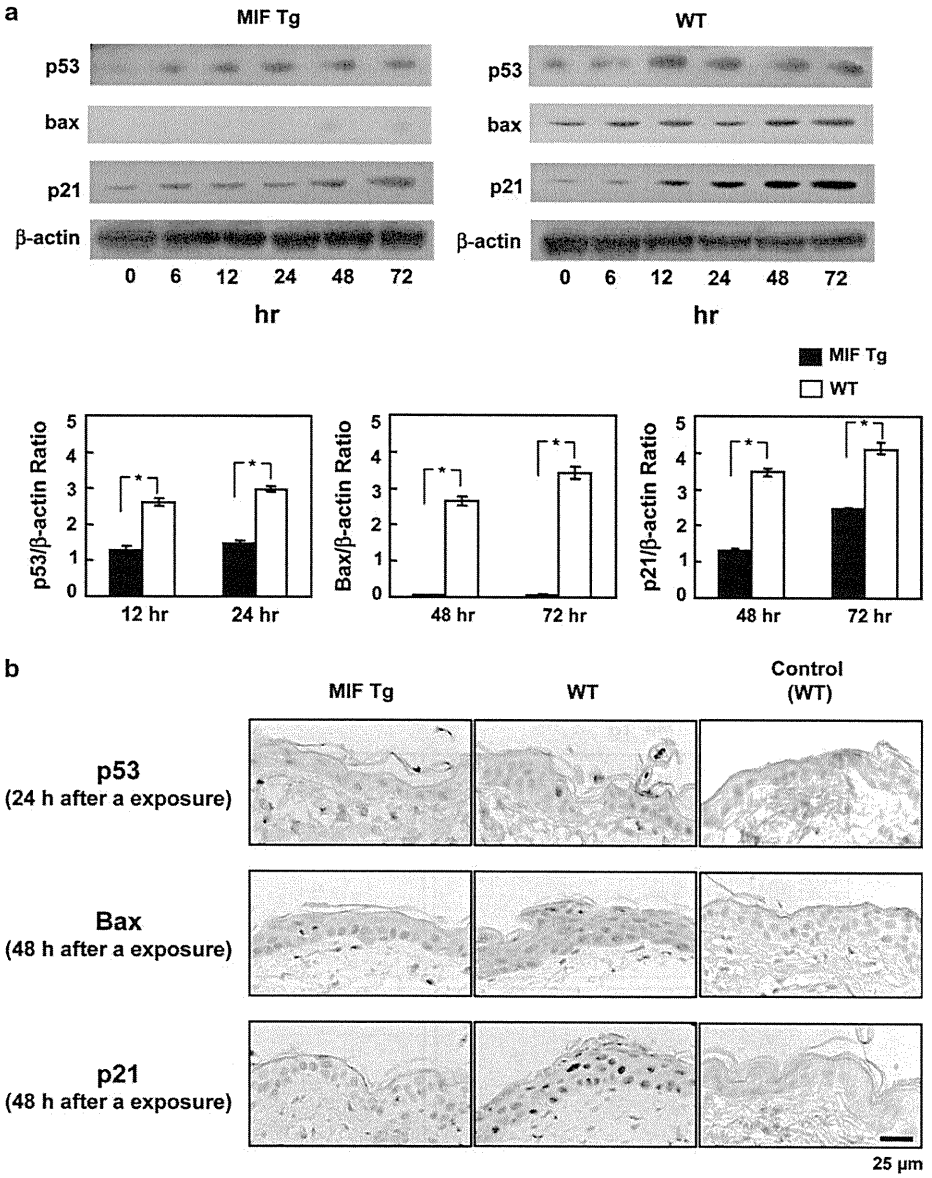

Fig. 5. p53, bax and p21 protein expression in UV-irradiated MIF Tg and WT mice epidermis. (**a**) Western blot analysis of p53, bax and p21 protein expression in unirradiated (0 h) and UVB-irradiated MIF Tg and WT mice skin at various time points. The relative amounts of protein associated with specific antibodies were normalized by the intensities of β-actin ($^{*}P < 0.0001$, $^{**}P < 0.001$, $n = 3$). The data shown are representative of three independent experiments. (**b**) Immunohistochemical analysis for p53, bax and p21 proteins in UVB-irradiated MIF Tg and WT mice skin at 24 h of p53 and at 48 h of bax and p21 immunoreactivity. This experiment was repeated three times with similar results. The scale bar indicates 25 μm.

Discussion

Chronic exposure to solar UV irradiation leads to photoaging, immunosuppression and ultimately carcinogenesis in the skin. Apoptosis and enhanced DNA repair are important p53-mediated responses (32). UVB-induced DNA lesions contribute to cell cycle arrest, DNA repair and finally apoptosis when DNA damage is beyond repair. p53/p21 are responsible for these adaptive protective responses. Moreover, p53 also directly participates in the initiation and regulation of the DNA repair procedure. Therefore, it is extremely important that apoptosis is induced quickly after UV irradiation, without any dysregulation. The current study demonstrated that an earlier onset of carcinogenesis and a higher incidence of tumors were observed in the MIF Tg mice compared with the WT mice after chronic UVB irradiation. In addition, the UVB-induced apoptosis of epidermal keratinocytes was inhibited in the MIF Tg mice. Significantly fewer TUNEL-positive cells were detected in MIF Tg mice in comparison with WT mice. There was a decreased expression of apoptosis-regulatory genes, p53, bax and p21 in MIF Tg mice after UVB irradiation in this study. A previous study has already confirmed that similar protective effects were observed in response to acute UVB light in the MIF Tg mice cornea (33). MIF is upregulated by UVB irradiation in mouse cornea and MIF Tg mice had less apoptotic cells. TUNEL staining in the cornea shows a significantly smaller number of TUNEL-positive nuclei in the MIF Tg mice compared with the WT mice after UV exposure (33).

MIF is a cytokine that not only plays a critical role in several inflammatory conditions but also inhibits p53-dependent apoptotic processes (23,24,34). Hudson *et al.* (23) reported that MIF

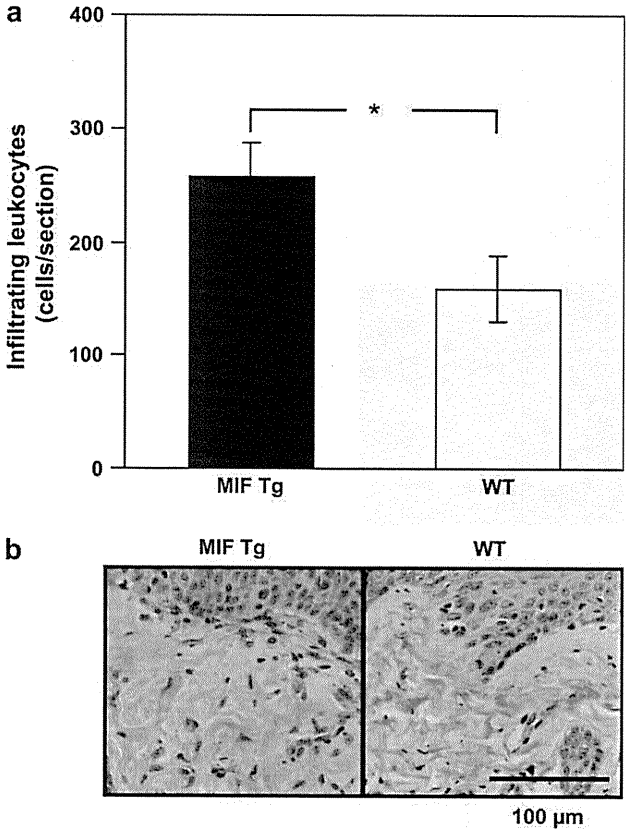

Fig. 6. UVB-induced cutaneous inflammation in MIF Tg and WT mice. (**a**) After three courses of UVB exposure, skin was obtained on day 7 and the paraffin-embedded skin samples (5 μm thick) were processed for routine hematoxylin and eosin staining following a standard protocol. Infiltrating leukocytes (monocyte/macrophages and neutrophils) of the MIF Tg mice were compared with the WT mice. Each value represents the mean ± SEM (n = 5). UVB exposure of MIF Tg mice resulted in greater leukocyte infiltration than that observed in UVB-irradiated WT mice skin (* $P < 0.05$). (**b**) Representative examples of micrographs of hematoxylin and eosin staining are shown from experiments conducted using skin samples (n = 5) that had identical patterns. Bar = 100 μm.

treatment was able to overcome p53 activity and inhibited its transcriptional activity. Recently, Martin *et al.* (35) reported that MIF-deficient mice showed significant increases in p53 activity following acute UVB irradiation, and MIF-deficient mice showed a reduction in tumor incidence in comparison with WT mice following chronic UVB exposure. Previous data from other groups and the current findings suggest that MIF has an inhibitory effect on UVB-induced photodamage by blocking the relevant expression of apoptosis-regulatory genes p53, bax and p21 and MIF plays an important role in UVB-induced tumor development and progression.

The present study also demonstrated that UVB exposure in MIF Tg mice resulted in greater leukocyte infiltration than that of the UVB-irradiated WT mice skin. UVB irradiation enhances the expression of MIF in the epidermis (25) and MIF Tg mice showed higher levels of MIF mRNA expression after UVB exposure in this study. UVB stimulates the production of several proinflammatory cytokines in the skin and these cytokines are known to be involved in the induction of skin carcinogenesis (11,36). For example, TNF-α is the essential cytokine in tumor promotion in mouse skin. Tumor promotion by 12-*O*-tetradecanoylphorbol-13-acetate on the skin of TNF-α-deficient mice decreased in comparison with WT mice. Similarly, tumor promotion in IL-6-deficient mice was significantly decreased by 12-*O*-tetradecanoylphorbol-13-acetate compared with the WT mice (11). UVB-induced inflammatory responses, such as the production of cytokines and the infiltration of inflammatory cells, are clearly linked to the development of skin tumors (3,4). The inhibition of this inflammatory response via topical application of an anti-inflammatory drug inhibits the acute inflammatory responses after UVB exposure and decreases tumor formation after chronic exposure (37). MIF has a direct proinflammatory role in inflammatory conditions and tumorigenesis (38). Once released, MIF acts as a proinflammatory cytokine to induce expression of other inflammatory cytokines, including IL-1, IL-6 and TNF-α. Therefore, intense inflammation in MIF Tg mice in response to UVB irradiation was found to correlate with the early onset of carcinogenesis and the higher incidence of tumors after chronic UVB irradiation.

MIF has a wider spectrum of action and exhibits proneoplastic activity. In many tumor cells and pretumor states, increased MIF mRNA can be detected in prostate (39), colon (40) and hepatocellular cancers (41), adenocarcinomas of the lung (42), glioblastomas (43) and melanomas (9). The role of MIF in proneoplastic activity has been examined by several groups. Fingerle *et al.* reported that embryonic fibroblasts from MIF deficient mice exhibit p53-dependent growth alterations, increased p53 transcriptional activity and resistance to ras-mediated transformation (23,24,34). Concurrent deletion of the p53 gene *in vivo* reversed the observed phenotype of cells deficient in MIF. *In vivo* studies showed that fibrosarcomas are smaller in size and have a lower mitotic index in MIF deficient mice relative to their WT counterparts. They concluded direct genetic evidence for a functional link between MIF and the p53 tumor suppressor (23,24,34). The effectiveness of an anti-MIF antibody on reducing tumor growth and neovascularization in lymphoma cells and vascular endothelial cells *in vivo* has been reported (22). Consistent with this finding, anti-MIF antibodies are effective in reducing tumor angiogenesis in melanoma cells (21). This was demonstrated *in vitro* by recombinant MIF in fibroblasts, where growth factor-induced stimulation of these cells resulted in increased MIF concentrations, activation of the ERK-MAP kinase pathway and a subsequent increase in cell proliferation (44). Meyer-Siegler *et al.* (45) has also shown that the addition of TGFβ results in increased MIF expression in a colon cancer cell line. Furthermore, Abe *et al.* (46) observed an increase in cytotoxic T lymphocytes following MIF inhibition as a result of specific antibodies. Moreover, the number of apoptotic tumor cells increased following MIF inhibition. Tumors arising in the MIF knockdown cells grew less rapidly and also showed an increased degree of apoptosis (47). These findings therefore suggest that once keratinocytes are mutated by UVB-induced DNA damage, they may develop into tumor cell, suggested that MIF has a dual role by promoting tumor cell growth and inhibiting the apoptotic processes.

In conclusion, chronic UVB irradiation induces early onset of skin carcinogenesis and the high incidence of tumors in MIF Tg mice. These findings suggest that chronic UVB exposure enhances MIF production, which may inhibit the p53-dependent apoptotic processes, enhance intensive inflammation and thereby induce photocarcinogenesis in the skin. Consequently, this newly identified mechanism may contribute to our overall understanding of photo-induced skin damage, which results in carcinogenesis. These findings are promising for the potential development of MIF inhibitors for therapeutic use and the treatment of photodamaged skin.

Funding

Ministry of Education, Science and Culture of Japan (No. 20591337).

Acknowledgements

Conflict of Interest Statement: None declared.

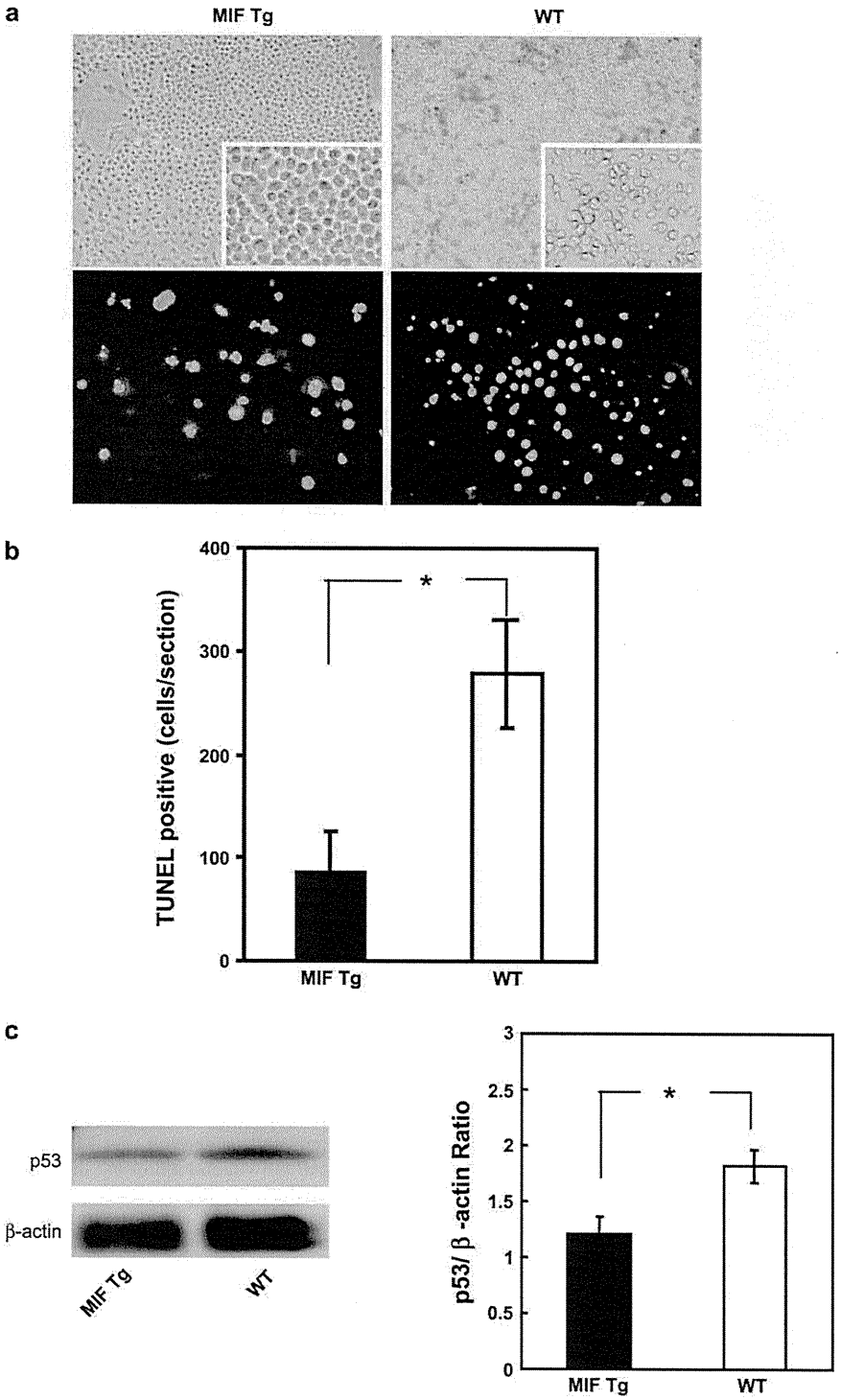

Fig. 7. UVB-induced apoptosis in cultured keratinocytes of MF Tg and WT. (**a**) Cultured keratinocyte from the MIF Tg or WT mice were irradiated with UVB at 50 mJ/cm^2. After 24 h, irradiated cells were analyzed for TUNEL assay. Upper panels indicate morphological pictures. Lower panels indicate TUNEL assay. (**b**) Apoptotic keratinocytes (TUNEL positive) from MIF Tg mice were significantly reduced compared with that of WT mice ($^*P < 0.005$). (**c**) p53 protein expression of UVB-irradiated keratinocytes were analyzed using western blot. The relative amounts of proteins associated with specific antibodies were normalized by the intensities of β-actin. These data shown are representative of three independent experiments. p53 expression of MIF Tg keratinocytes was lower than that of WT mice ($^*P < 0.005$).

References

1. Young,A.R. (1990) Cumulative effects of ultraviolet radiation on the skin: cancer and photoaging. *Semin. Dermatol.*, **9**, 25–31.
2. Kraemer,K.H. (1997) Sunlight and skin cancer: another link revealed. *Proc. Natl Acad. Sci. USA*, **94**, 11–14.
3. Fischer,S.M. *et al.* (1999) Chemopreventive activity of celecoxib, a specific cyclooxygenase-2 inhibitor, and indomethacin against ultraviolet light-induced skin carcinogenesis. *Mol. Carcinog.*, **25**, 231–240.
4. Pentland,A.P. *et al.* (1999) Reduction of UV-induced skin tumors in hairless mice by selective COX-2 inhibition. *Carcinogenesis*, **20**, 1939–1944.
5. Cleaver,J.E. *et al.* (2002) UV damage, DNA repair and skin carcinogenesis. *Front Biosci.*, **7**, d1024–d1043.
6. Stenback,F. *et al.* (1998) p53 expression in skin carcinogenesis and its relationship to cell proliferation and tumour growth. *Eur. J. Cancer*, **34**, 1415–1424.
7. Ansel,J.C. *et al.* (1988) The expression and modulation of IL-1 alpha in murine keratinocytes. *J. Immunol.*, **140**, 2274–2278.
8. Kupper,T.S. *et al.* (1987) Interleukin 1 gene expression in cultured human keratinocytes is augmented by ultraviolet irradiation. *J. Clin. Invest.*, **80**, 430–436.
9. Kirnbauer,R. *et al.* (1991) Regulation of epidermal cell interleukin-6 production by UV light and corticosteroids. *J. Invest. Dermatol.*, **96**, 484–489.
10. Kock,A. *et al.* (1990) Human keratinocytes are a source for tumor necrosis factor alpha: evidence for synthesis and release upon stimulation with endotoxin or ultraviolet light. *J. Exp. Med.*, **172**, 1609–1614.
11. Suganuma,M. *et al.* (2002) Discrete roles of cytokines, TNF-alpha, IL-1, IL-6 in tumor promotion and cell transformation. *Int. J. Oncol.*, **20**, 131–136.
12. Bloom,B.R. *et al.* (1966) Mechanism of a reaction *in vitro* associated with delayed-type hypersensitivity. *Science*, **153**, 80–82.
13. David,J.R. (1966) Delayed hypersensitivity *in vitro*: its mediation by cell-free substances formed by lymphoid cell-antigen interaction. *Proc. Natl Acad. Sci. USA*, **56**, 72–77.
14. Bernhagen,J. *et al.* (1993) MIF is a pituitary-derived cytokine that potentiates lethal endotoxaemia. *Nature*, **365**, 756–759.
15. Calandra,T. *et al.* (1994) The macrophage is an important and previously unrecognized source of macrophage migration inhibitory factor. *J. Exp. Med.*, **179**, 1895–1902.
16. Lanahan,A. *et al.* (1992) Growth factor-induced delayed early response genes. *Mol. Cell Biol.*, **12**, 3919–3929.
17. Wistow,G.J. *et al.* (1993) A macrophage migration inhibitory factor is expressed in the differentiating cells of the eye lens. *Proc. Natl Acad. Sci. USA*, **90**, 1272–1275.
18. Bucala,R. (1996) MIF re-discovered: pituitary hormone and glucocorticoid-induced regulator of cytokine production. *Cytokine Growth Factor Rev.*, **7**, 19–24.
19. Bacher,M. *et al.* (1997) Migration inhibitory factor expression in experimentally induced endotoxemia. *Am. J. Pathol.*, **150**, 235–246.
20. Nishihira,J. (2000) Macrophage migration inhibitory factor (MIF): its essential role in the immune system and cell growth. *J. Interferon Cytokine Res.*, **20**, 751–762.
21. Shimizu,T. *et al.* (1999) High expression of macrophage migration inhibitory factor in human melanoma cells and its role in tumor cell growth and angiogenesis. *Biochem. Biophys. Res. Commun.*, **264**, 751–758.
22. Chesney,J. *et al.* (1999) An essential role for macrophage migration inhibitory factor (MIF) in angiogenesis and the growth of a murine lymphoma. *Mol. Med.*, **5**, 181–191.
23. Hudson,J.D. *et al.* (1999) A proinflammatory cytokine inhibits p53 tumor suppressor activity. *J. Exp. Med.*, **190**, 1375–1382.
24. Nemajerova,A. *et al.* (2007) Impaired DNA damage checkpoint response in MIF-deficient mice. *EMBO J.*, **26**, 987–997.
25. Shimizu,T. *et al.* (1999) Ultraviolet B radiation upregulates the production of macrophage migration inhibitory factor (MIF) in human epidermal keratinocytes. *J. Invest. Dermatol.*, **112**, 210–215.
26. Watanabe,H. *et al.* (2004) Ultraviolet A-induced production of matrix metalloproteinase-1 is mediated by macrophage migration inhibitory factor (MIF) in human dermal fibroblasts. *J. Biol. Chem.*, **279**, 1676–1683.
27. Shimizu,T. *et al.* (1997) Macrophage migration inhibitory factor is an essential immunoregulatory cytokine in atopic dermatitis. *Biochem. Biophys. Res. Commun.*, **240**, 173–178.
28. Sasaki,S. *et al.* (2004) Transgene of MIF induces podocyte injury and progressive mesangial sclerosis in the mouse kidney. *Kidney Int.*, **65**, 469–481.
29. Akagi,Y. *et al.* (1997) Transcriptional activation of a hybrid promoter composed of cytomegalovirus enhancer and beta-actin/beta-globin gene in glomerular epithelial cells *in vivo*. *Kidney Int.*, **51**, 1265–1269.
30. Noonan,F.P. *et al.* (2000) Accelerated ultraviolet radiation-induced carcinogenesis in hepatocyte growth factor/scatter factor transgenic mice. *Cancer Res.*, **60**, 3738–3743.
31. Arad,S. *et al.* (2008) Topical thymidine dinucleotide treatment reduces development of ultraviolet-induced basal cell carcinoma in Ptch-1+/- mice. *Am. J. Pathol.*, **172**, 1248–1255.
32. Levine,A.J. (1997) p53, the cellular gatekeeper for growth and division. *Cell*, **88**, 323–331.
33. Kitaichi,N. *et al.* (2008) Macrophage migration inhibitory factor ameliorates UV-induced photokeratitis in mice. *Exp. Eye Res.*, **86**, 929–935.
34. Fingerle-Rowson,G. *et al.* (2003) The p53-dependent effects of macrophage migration inhibitory factor revealed by gene targeting. *Proc. Natl Acad. Sci. USA*, **100**, 9354–9359.
35. Martin,J. *et al.* (2008) Macrophage migration inhibitory factor (MIF) plays a critical role in pathogenesis of ultraviolet-B (UVB) -induced nonmelanoma skin cancer (NMSC). *FASEB J.*, **23**, 720–730.
36. Moore,R.J. *et al.* (1999) Mice deficient in tumor necrosis factor-alpha are resistant to skin carcinogenesis. *Nat. Med.*, **5**, 828–831.
37. Wilgus,T.A. *et al.* (2003) Inhibition of cutaneous ultraviolet light B-mediated inflammation and tumor formation with topical celecoxib treatment. *Mol. Carcinog.*, **38**, 49–58.
38. Bach,J.P. *et al.* (2008) Role of MIF in inflammation and tumorigenesis. *Oncology*, **75**, 127–133.
39. Meyer-Siegler,K. *et al.* (1998) Expression of macrophage migration inhibitory factor in the human prostate. *Diagn. Mol. Pathol.*, **7**, 44–50.
40. Legendre,H. *et al.* (2003) Prognostic values of galectin-3 and the macrophage migration inhibitory factor (MIF) in human colorectal cancers. *Mod. Pathol.*, **16**, 491–504.
41. Ren,Y. *et al.* (2003) Macrophage migration inhibitory factor: roles in regulating tumor cell migration and expression of angiogenic factors in hepatocellular carcinoma. *Int. J. Cancer*, **107**, 22–29.
42. Kamimura,A. *et al.* (2000) Intracellular distribution of macrophage migration inhibitory factor predicts the prognosis of patients with adenocarcinoma of the lung. *Cancer*, **89**, 334–341.
43. Rogge,L. (2002) A genomic view of helper T cell subsets. *Ann. N. Y. Acad. Sci.*, **975**, 57–67.
44. Takahashi,N. *et al.* (1998) Involvement of macrophage migration inhibitory factor (MIF) in the mechanism of tumor cell growth. *Mol. Med.*, **4**, 707–714.
45. Meyer-Siegler,K.L. *et al.* (2006) Inhibition of macrophage migration inhibitory factor or its receptor (CD74) attenuates growth and invasion of DU-145 prostate cancer cells. *J. Immunol.*, **177**, 8730–8739.
46. Abe,R. *et al.* (2001) Regulation of the CTL response by macrophage migration inhibitory factor. *J. Immunol.*, **166**, 747–753.
47. Hagemann,T. *et al.* (2007) Ovarian cancer cell-derived migration inhibitory factor enhances tumor growth, progression, and angiogenesis. *Mol. Cancer Ther.*, **6**, 1993–2002.

Received March 2, 2009; revised June 15, 2009; accepted June 20, 2009

parapoxviruses and the identification of a 39 kDa immunodominant protein. *Arch Virol* 1998; **143**: 2289–303.
5 Torfason EG, Gunadottir S. Polymerase chain reaction for laboratory diagnosis of orf virus infections. *J Clin Virol* 2002; **24**: 79–84.

Melanonychia caused by *Stenotrophomonas maltophilia*

doi: 10.1111/j.1365-2230.2008.02752.x

Subungual melanomas often present initially as brown to black nail pigmentation, thus it is important to make a precise diagnosis in cases of melanonychia. Infection or colonization with bacteria or fungi is also known to cause melanonychia.[1] We describe a case of melanonychia caused by *Stenotrophomonas maltophilia* that was suspected to be melanoma.

A 54-year-old man was referred with a 1-year history of an enlarging area of pigmentation in the right great toenail. He was in good health and was taking no medication.

On examination, the great toe nail on his right foot showed partial thickening, onycholysis and irregular pigmentation over most of the nail plate (Fig. 1). Pigmentation of the proximal or lateral nail folds (Hutchinson's sign) was not observed.

Microscopy with potassium hydroxide showed no fungal component in the nail specimen. An excisional biopsy specimen was taken from the pigmented portion of the nail and underlying nail bed showed a large number of Gram-negative bacilli and dark-brown to black pigmentation within the nail plate. The pigmentation in the section disappeared after melanin digestion. Neither melanocyte proliferation nor hypermelanosis was observed in the underlying hyponychium.

Bacterial culture from the nail samples grew *S. maltophilia*, although fungal culture was negative. From these findings, the diagnosis of melanonychia due to *S. maltophilia* was established. After the resection operation, there was no further recurrence of nail pigmentation.

Melanonychia may be due to exogenous substances including bacterial, mycotic and blood pigments, or endogenous melanin pigmentation.[1–3] Bacterial pigmentation, most commonly due to *Pseudomonas aeruginosa* or *Proteus* spp., has a greenish or greyish hue.[2] However, in the present case, the colour was almost black. Melanocytic lesions were excluded by the excisional biopsy of the pigmented nail plate and underlying hyponychium, and the patient was diagnosed with melanonychia due to *S. maltophilia*.

To our knowledge, this is the first case report of melanonychia caused by *S. maltophilia*. *Stenotrophomonas maltophilia* is a nonfermentative Gram-negative bacillus found in various environments such as water, soil, plants and food and in hospitals.[4] *Stenotrophomonas maltophilia* has emerged as an important pathogen capable of causing a broad spectrum of clinical syndromes including pneumonia, bacterial sepsis, urinary tract infections, endocarditis, meningitis and a variety of skin presentations including cellulitis, erythematous nodules, skin ulcers and acral necrosis.[4] *Stenotrophomonas maltophilia* is known to express the tyrosinase gene *mel* and has been shown to

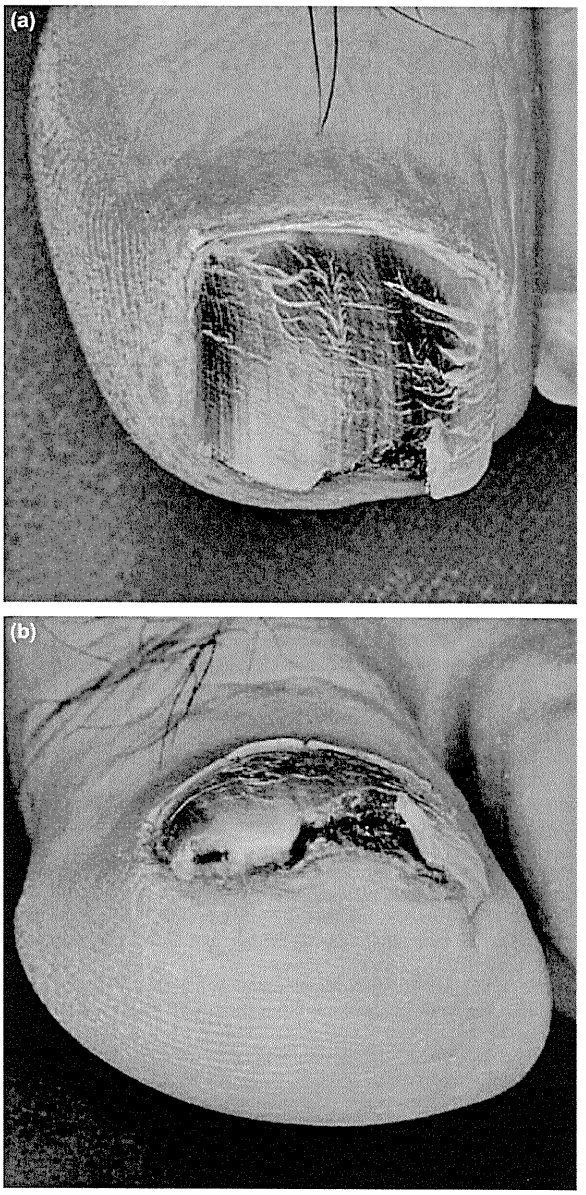

Figure 1 Black discoloration of the first toe nail on the right foot. (a) The thickened, partly onycholytic nail plate with the intact nail fold. The distal portion of the nail had been cut into sections. (b) Pigmentation, mainly in the nail plate but also on the nail bed.

produce melanin.[5] Production of melanin is thought to be linked to protection against environmental insults such as antibiotics.[6] The melanin derived from *S. maltophilia* probably contributed to the pigmentation of the nail plate in this case. Melanonychia caused by *S. maltophilia* may be misdiagnosed as a melanocytic lesion, because a Fontana–Masson stain is positive for nail melanin pigmentation due to *S. maltophilia*, which differs from the fluorescein and pyocyanin pigmentation due to *Pseudomonas aeruginosa*. The present case suggests that non-*Pseudomonas aeruginosa* bacteria such as *S. maltophilia* should be included in the list of causes of a black nail.

E. Hamasaka, M. Akiyama, H. Hata, S. Aoyagi and H. Shimizu
Department of Dermatology, Hokkaido University Graduate School of Medicine, North 15 West 7, Kita-ku, Sapporo 060-8638, Japan
E-mail: akiyama@med.hokudai.ac.jp
Conflict of interest: none declared.
Accepted for publication 12 November 2007

References

1 Braun RP, Baran R, Le Gal FA *et al.* Diagnosis and management of nail pigmentations. *J Am Acad Dermatol* 2007; **56**: 835–47.
2 Haneke E, Baran R. Longitudinal melanonychia. *Dermatol Surg* 2001; **27**: 580–4.
3 Parlak AH, Goksugur N, Karabay O. A case of melanonychia due to Candida albicans. *Clin Exp Dermatol* 2006; **31**: 398–400.
4 Nicodemo AC, Garcia Paez JI. Antimicrobial therapy for *Stenotrophomonas maltophilia infections. Eur J Clin Microbiol Infect Dis* 2007; **26**: 229–37.
5 Wang G, Aazaz A, Peng Z, Shen P. Cloning and overexpression of a tyrosinase *gene mel from Pseudomonas maltophila. FEMS Microbiol Lett* 2000; **185**: 23–7.
6 Tan C-K, Liaw S-J, Yu C-J *et al.* Extensively drug-resistant. Stenotrophomonas maltophilia in a tertiary care hospital inn Taiwan: microbiologic characteristics, clinical features, and outcomes. *Diagn Microbiol Infect Dis* 2008; **60**: 205–10.

A case of solitary collagenoma localized on the upper lip mimicking mucocele

doi: 10.1111/j.1365-2230.2008.02754.x

Collagenomas are rare hamartomatous malformations of the dermis, characterized by a proliferation of normal collagen tissue. We present a case of isolated (solitary) collagenoma arising in the upper lip, an uncommon location for this disease, and clinically mimicking mucocele.

A 56-year-old Japanese woman was referred to us with a 3-month history of an asymptomatic soft mass on the left upper lip. She was otherwise in good health. Her medical history was not relevant, and there was no family history of a similar disorder.

Physical examination found a slightly raised, soft, elastic, bluish-white nodule on the inner surface of the left upper labial mucosa (Fig. 1). The lesion was well demarcated, and measured 5 mm in diameter with a round shape and smooth surface. No lesions were observed on the trunk, limbs or any other body sites.

Because of the suspicion of mucocele, an excisional skin biopsy was taken for both diagnostic and therapeutic purposes. Histopathological examination found an increased number of collagen bundles in the dermis, which were arranged randomly (Fig. 2a). The collagen bundles stained strongly with Azan–Mallory stain, showing an intense blue colour (Fig. 2b). The lesion had no capsule and was relatively well-defined. Elastic van Gieson stain showed a mild decrease in elastic bundles. Based on the histopathological findings, a diagnosis of solitary collagenoma was made.

Collagenomas, also known as connective tissue naevi of the skin (hamartomas), are composed predominantly of collagen. According to the classification of the genetic inheritance pattern, they are classified as either inherited or acquired.[1,2] The inherited group includes familial cutaneous collagenoma and shagreen patches of tuberous sclerosis, which are inherited in an autosomal dominant matter. The acquired group includes eruptive collagenomas and isolated collagenomas. In both familial and eruptive collagenomas, lesions are characterized clinically by asymptomatic, multiple, skin-coloured papules and nodules distributed symmetrically on the trunk and upper arms.[1,2] In contrast, isolated collagenoma is sporadic, localized to only one body region, and not associated with any disease.

In our patient, the diagnosis of isolated collagenoma, rather than eruptive collagenoma, was made because the lesion was a solitary nodule on the lip, and the patient had no family history of the condition.

The aetiology of collagenomas is still unknown. However, acquired collagenomas occur commonly on trauma-

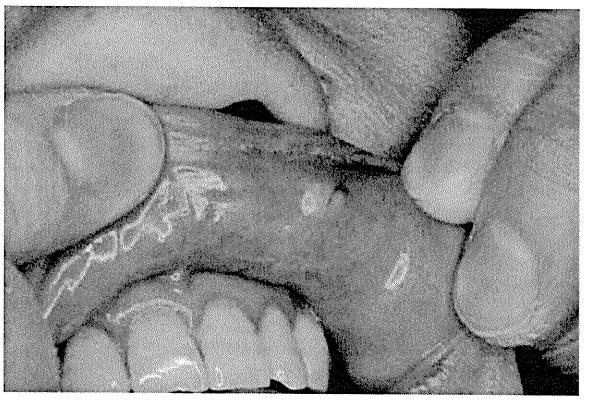

Figure 1 A bluish-white nodule mimicking a mucocele on the inner mucosa of the upper lip.

DNA vaccination against macrophage migration inhibitory factor improves atopic dermatitis in murine models

Asuka Hamasaka, MD,[a] Riichiro Abe, MD, PhD,[a] Yoshikazu Koyama, PhD,[b] Naoya Yoshioka, MS,[a] Yasuyuki Fujita, MD,[a] Daichi Hoshina, MD,[a] Mikako Sasaki, MS,[a] Tsutomu Hirasawa, PhD,[c] Shin Onodera, MD, PhD,[d] Shigeki Ohshima, MD, PhD,[e] Lin Leng, PhD,[f] Richard Bucala, MD, PhD,[f] Jun Nishihira, MD, PhD,[b] Tadamichi Shimizu, MD, PhD,[g] and Hiroshi Shimizu, MD, PhD[a] *Sapporo, Ebetsu, Osaka, and Toyama, Japan, and New Haven, Conn*

Background: Atopic dermatitis (AD) is a common chronic inflammatory skin disease. Macrophage migration inhibitory factor (MIF) is a proinflammatory cytokine that has been implicated in the pathogenesis of AD. Recently, we developed a novel DNA vaccine that generates neutralizing endogenous anti-MIF antibodies.

Objective: This study explores the preventive and therapeutic effects of this MIF-DNA vaccine in mouse models of AD.

Methods: Two different AD model mice (DS-Nh and NC/Nga) received MIF-DNA vaccination to analyze preventive and therapeutic effects, as assessed by clinical skin scores, histologic findings, and serum IgE levels.

Results: In murine models of AD, MIF-DNA vaccination prevented the occurrence of the AD skin phenotype. Furthermore, administration of MIF-DNA vaccine to mice that had already developed AD produced a rapid improvement in AD skin manifestation. There were reduced histologic signs of inflammation and lower serum IgE levels in treated mice compared with those seen in control animals. Finally, passive transfer of IgG from MIF-DNA vaccinated mice to AD mice also produced a significant therapeutic effect. These results demonstrate that MIF-DNA vaccination not only prevents the development of AD but also improves the symptoms of pre-existing AD.

Conclusion: Taken together, the induction of an anti-MIF autoantibody response using MIF-DNA vaccination appears to be a useful approach in the treatment of AD. (J Allergy Clin Immunol 2009;124:90-9.)

Key words: *Atopic dermatitis, macrophage migration inhibitory factor, DNA vaccination*

Abbreviations used
AD: Atopic dermatitis
MIF: Macrophage migration inhibitory factor
TTX: Tetanus toxin P30 T_H epitope

Atopic dermatitis (AD) is a chronic, relapsing inflammatory skin disease with significant morbidity and an adverse effect on patient well-being.[1] The prevalence of AD has increased 2- to 3-fold during the past 3 decades in industrialized countries, and it presently occurs in 10% to 20% of children and 1% to 3% of adults.[2] AD is thought to result from a dysregulation in the normal interaction between the environment, genes, defects in skin barrier function, and systemic and local immunologic responses.[3] The contribution of the immune response to the pathogenesis of AD has been largely attributed to abnormalities in the adaptive immune system, with key roles played by T_H1/T_H2 cell dysregulation, IgE production, dendritic cell signaling, and mast cell hyperactivity, leading to the pruritic inflammatory dermatosis that characterizes AD.[3]

Macrophage migration inhibitory factor (MIF) is an upstream regulator of the inflammatory response, and it is upregulated in various inflammatory disorders, including AD.[4] We previously reported that serum MIF levels in patients with AD were significantly increased compared with those seen in healthy control subjects and patients without AD.[5] In addition, circulating MIF levels in patients with AD decrease as the clinical features of the disease improve, suggesting that MIF might play a pivotal role in the inflammatory response in these patients.[5,6] Moreover, MIF promotes IL-2 and IL-2 receptor expression and memory T-cell development, and it might influence T_H1/T_H2 cell differentiation responses.[6,7] Based on these observations suggesting that MIF might be a therapeutic target in AD, we hypothesized that inhibition of MIF with neutralizing antibodies might induce beneficial therapeutic effects in patients with AD.

Monoclonal antibodies directed against proinflammatory cytokines, such as TNF-α, have been used for the treatment of rheumatoid arthritis, Crohn disease, and psoriasis,[8-10] and there have been a few reports describing the use of anti–TNF-α mAbs for the treatment of AD.[7,8] The application of mAbs to AD nevertheless might be difficult because of the requirement for frequent injections, the large quantities of immunoglobulin protein required, and the associated costs of production. Moreover, even fully humanized antibodies are potentially immunogenic and might elicit antibody responses, thereby limiting their long-term therapeutic efficacy. These limitations have led to the development of alternative neutralization strategies, including methods that aim to elicit autoantibodies against target proteins,

From the Departments of [a]Dermatology, [d]Sports Medicine and Joint Reconstruction Surgery, and [c]Orthopedics, Hokkaido University Graduate School of Medicine, Sapporo; [b]the Department of Medical Information, Hokkaido Information University, Ebetsu; [c]Discovery Research Laboratories, Shionogi and Co Ltd, Osaka; [f]the Department of Medicine, and Pathology, Yale University School of Medicine, New Haven; and [g]the Department of Dermatology, Graduate School of Medicine and Pharmaceutical Sciences, University of Toyama, Toyama.

Disclosure of potential conflict of interest: R. Bucala receives grant support from the National Institutes of Health, the Alliance for Lupus Research, and Promedior. The rest of the authors have declared that they have no conflict of interest.

Received for publication November 5, 2008; revised April 13, 2009; accepted for publication April 14, 2009.

Available online June 1, 2009.

Reprint requests: Riichiro Abe, MD, PhD, or Hiroshi Shimizu, MD, PhD, Department of Dermatology, Hokkaido University Graduate School of Medicine, Sapporo 060-8638, Japan. E-mail: aberi@med.hokudai.ac.jp and shimizu@med.hokudai.ac.jp.

0091-6749/$36.00

doi:10.1016/j.jaci.2009.04.025

such as cytokines or pathogens, by administering them in a naked or partially modified form as therapeutic vaccines.

We recently developed an MIF-DNA vaccine that breaks immunologic tolerance by introducing oligonucleotides encoding a foreign T_H cell epitope into the murine MIF cDNA sequence.[11,12] We demonstrated that this MIF-DNA vaccination elicits production of endogenous anti-MIF antibodies and showed a significant amelioration of symptoms in murine models of rheumatoid arthritis[9] and sepsis.[10]

The present study describes for the first time the preventive and therapeutic effects of this MIF-DNA vaccine in 2 different mouse models of AD.

METHODS

Animals

Six-week-old female BALB/c mice were purchased from Japan Clea (Shizuoka, Japan). Male DS-Nh mice were provided by Aburabi Laboratories, Shionogi and Co, Ltd (Shiga, Japan), and male NC/Nga mice were purchased from SLC (Hamamatsu, Japan). All mice were bred and housed under conventional conditions, and procedures were conducted according to the guidelines of the Hokkaido University Institutional Animal Care and Use Committee under an approved protocol.

Production of DNA vaccine

We previously reported the design of the MIF/tetanus toxin P30 T_H epitope (TTX) DNA expression plasmid and our analysis of the *in vitro* expression of MIF/TTX by using this plasmid.[11] For the generation of immunologically active MIF antigen, an MIF construct harboring a T_H epitope at its second loop region was designed. For that purpose, the coding region for the second loop of the mouse MIF, amino acids 32 to 37 (GKPAQY), was deleted from the MIF cDNA and substituted with an *Eco*RI site. A complementary DNA coding for the TTX (FNNFTVSFWLRVPKVSASHL) with *Eco*RI sites at both termini was obtained by means of hybridization of partially overlapping oligo DNAs (sense, ggaattcaacaacttcaccgtgagcttctggctgcgcgtgcccaa; antisense, ggaattccaggtggctggcgctcaccttgggcacgcgcagccaga) after polymerization with the Klenow fragment of DNA polymerase. After digestion with *Eco*RI, the cDNA coding for the P30 T_H epitope was inserted into the *Eco*RI site of the MIF expression plasmid lacking the second loop, and a clone with the insert of correct orientation was selected. For vaccination, the plasmid DNA was purified by using standard methods with alkaline lysis followed by 2 rounds of CsCl density gradient ultracentrifugation.

Vaccination protocols

Gene transfer into muscle by means of electroporation was performed as described previously.[11] Briefly, mice were anesthetized with ether and shaved near their hind legs. A pair of electrode needles (5-mm gap and 0.5-mm diameter; NEPA GENE, Chiba, Japan) was then inserted into an anterior tibial muscle, and DNA vaccine (25 μg/25 μL of 0.9% saline) was injected into the portion between the needles. Electrical pulses (50 V, 50 ms, 3 times) were applied (T820 and Optimizer 500; BTX, San Diego, Calif) and followed by another 3 pulses with inverted polarity. The same injection and electroporation was applied to the other tibial muscle. Thus 50 μg of the naked plasmid was injected per mouse into the tibias. A similar vaccination was repeated 3 weeks later.

Evaluation of anti-MIF antibody titer in sera of DNA-vaccinated mice

Anti-MIF titers in plasma were determined by means of direct ELISA. Briefly, individual plasma from vaccinated mice were collected from the tail vein and diluted with 0.1% BSA/PBS/0.05% Tween 20. Small aliquots of diluted plasma (1:200) were added into 96-well flat-bottom plates precoated with recombinant MIF. Anti-MIF antibodies that reacted with the precoated recombinant MIF were detected with goat anti-mouse antibody conjugated with horseradish peroxidase, followed by color development with substrate reagent (Techne, Minneapolis, Minn).

Evaluation of clinical skin severity score

Mice were macroscopically observed and scored by 2 persons blind to the treatment protocol. Before skin conditions were scored, scratching behavior was observed for 2 minutes. A total clinical severity for AD-like lesions was defined as the sum of the individual scores graded as 0 (none), 1 (mild), 2 (moderate), and 3 (severe) for each of 5 signs and symptoms (itch, erythema, edema, excoriation/erosion, and scaling/dryness).[13]

Measurement of IgE and TNF-α levels in sera

Serum total IgE levels were measured by using a sandwich ELISA kit (Yamasa Shouyu, Chiba, Japan). Serum MIF levels were assayed with ELISA kits for Genetic Lab (Sapporo, Japan). The ELISA procedures were conducted according to the manufacturer's instructions. The concentration of TNF-α was determined by using the BD Cytometric Bead Array (BD PharMingen, San Jose, Calif). Flow cytometric analysis was carried out with a FACSCalibur flow cytometer (Becton Dickinson, Mountain View, Calif).

Real-time PCR analysis

Total RNA was extracted from dorsal skin to quantify cytokine mRNA expression levels in dermatitis lesions. RNA samples were analyzed with the ABI prism 7000 sequence detection system (Applied Biosystems, Foster City, Calif). Primers and probes specific for IL-1β, IL-4, IL-6, and IFN-γ were obtained from the TaqMan gene expression assay (Applied Biosystems). Differences between the mean cycle threshold (CT) values of cytokines and those of β-actin (Applied Biosystems) were calculated as

$$\Delta CT_{sample} = CT_{cytokine} - CT_{\beta-actin},$$

and those of ΔCT for the normal adult skin were calculated as

$$\Delta CT_{calibrator} = CT_{cytokine} - CT_{\beta-actin}.$$

Final results for fetal skin sample/adult skin (as percentages) were determined as $2-(\Delta CT_{sample} - \Delta CT_{calibrator})$.

Histologic analysis

Six-micrometer-thick sections of dorsal skin were stained with hematoxylin and eosin, acidic toluidine blue (pH 4.0) for mast cells, and direct fast scarlet for eosinophils. Cells between the epithelium and panniculus carnosus were counted at a magnification of ×400 and were expressed as the total number of cells in 5 fields.

Treatment of neutralizing MIF mAbs

Neutralizing anti-MIF mAb (NIH-III.D9) was previously described.[14] Neutralizing MIF mAbs (50 μg) or control IgG (50 μg) were injected intravenously into 15-week-old NC/Nga mice with dermatitis twice a week for 3 weeks.

Adoptive transfer of autoantibodies elicited by DNA vaccines

IgG was purified from the sera of control pCAGGS plasmid– or MIF/TTX-vaccinated DS mice at 6 weeks after the vaccination by using the protein A Antibody Purification Kit (Amersham Biosciences, Piscataway, NJ). The purified IgG was tested for its ability to suppress ongoing dermatitis in an adoptive transfer experiment. DS-Nh mice with developing dermatitis were separated at 15 weeks of age into 3 equally sick groups of 3 mice each. Every 3 days, these animals were administered 50 μg per mouse of purified IgG from control pCAGGS plasmid–vaccinated DS-Nh mice, purified IgG from MIF/TTX-vaccinated DS-Nh mice, or an equal volume of PBS.

RESULTS

MIF/TTX vaccination prevents the onset of AD in DS-Nh mice

DS-Nh mice housed under conventional conditions but not in a specific pathogen free environment spontaneously exhibit AD-like skin symptoms, including erythema, edema, excoriation, erosion, dry skin, and desquamation.[15-17] Early skin symptoms appear around 9 weeks of age and continue to worsen until age 25 weeks. An increase in total serum IgE levels is detected at approximately 17 weeks of age and after the development of skin lesions.[15-17]

We first examined the potential protective effect of the MIF/TTX vaccine on dermatitis development by treating 9-week-old DS-Nh mice before the development of skin eruptions. The clinical features of the control pCAGGS plasmid–vaccinated mice were similar to those of untreated mice. At 18 weeks of age, or 9 weeks after the vaccination, both groups of mice showed severe erythema, erosions, and dry skin (Fig 1, *A*). By contrast, the MIF/TTX-vaccinated mice exhibited almost no eruptions (Fig 1, *B*). The clinical skin score of MIF/TTX-vaccinated mice was low until 21 weeks of age (Fig 1, *C*), which is a time at which the MIF/TTX-vaccinated mice showed high serum levels of anti-MIF antibodies (Fig 1, *D*). Furthermore, in the MIF/TTX-vaccinated mice the serum level of IgE was significantly decreased and the serum MIF level was only slightly decreased when compared with those seen in the control vaccinated mice (Fig 1, *E* and *F*). In addition, cytokine expression in affected skin lesions was analyzed by using real-time PCR. The T_H2 cytokine IL-4 was very slightly downregulated, and the T_H1 cytokine IFN-γ was slightly upregulated. Of note, the expression of the proinflammatory cytokines IL-1β and IL-6 was significantly suppressed in MIF-vaccinated mice compared with that seen in control mice (Fig 1, *G*). Therefore the inhibition of MIF in the atopic model mice appears to result primarily in the suppression of inflammation rather than affecting the T_H1/T_H2 cytokine balance.

Improvement of clinical skin condition with MIF/TTX vaccine also was confirmed by the observation that the lesions of mice vaccinated with MIF/TTX vaccine showed amelioration in hyperkeratosis, acanthosis, dermal edema, and infiltration of the inflammatory cells at 21 weeks when compared with the condition of mice vaccinated with control pCAGGS plasmid (Fig 2, *A*). At the affected skin sites, the numbers of eosinophils and mast cells decreased significantly in the MIF/TTX-vaccinated mice at 21 weeks when compared with those seen in the control vaccinated mice (Fig 2, *B-D*).

These data clearly show that MIF/TTX vaccination can prevent the onset of AD-like dermatitis in DS-Nh mice.

MIF/TTX vaccination improves pre-existing AD

To determine whether the MIF/TTX vaccine has any therapeutic effect in AD, we next vaccinated 15-week-old DS-Nh mice with pre-existing AD and evaluated the progression of skin changes. Mice treated with the control plasmid continued to exhibit severe dermatitis 6 weeks after vaccination (Fig 3, *A*). By contrast, the MIF/TTX vaccination significantly improved dermatitis symptoms (Fig 3, *B*). The clinical skin scores of control-vaccinated mice increased after the vaccination, whereas that of MIF/TTX-vaccinated mice began to decrease at 21 weeks of age (Fig 3, *C*). At this time, the MIF/TTX-vaccinated mice showed high levels of anti-MIF antibodies (Fig 3, *D*). Furthermore, the serum IgE and MIF levels of MIF/TTX-vaccinated mice also were lower than those of control mice at 21 weeks of age (Fig 3, *E* and *F*). In addition, serum TNF-α levels were significantly lower in the MIF/TTX-vaccinated mice when compared with those seen in the control plasmid–vaccinated mice (Fig 3, *G*).

By means of histologic analysis, the lesions of mice vaccinated with MIF/TTX vaccine showed improvement of hyperkeratosis, acanthosis, dermal edema, and infiltration of inflammatory cells at 21 weeks when compared with the control plasmid–vaccinated mice (Fig 4, *A*). In addition, the numbers of eosinophils and mast cells decreased significantly in the MIF/TTX-vaccinated mice at 21 weeks when compared with those seen in the control mice (Fig 4, *B-D*). The serum IgE level of MIF/TTX-vaccinated mice decreased at 21 weeks of age compared with that of control-vaccinated mice (Fig 4, *E*).

These data indicate that MIF/TTX vaccination leads to an improvement in already established dermatitis in the DS-Nh mice.

We further observed that MIF-DNA vaccine improved the manifestation of pre-existing AD in a second model of AD, which develops in the NC/Nga strain.[11,13] We vaccinated 15-week-old NC/Nga mice with dermatitis, and although the control pCAGGS plasmid–vaccinated mice still had severe dermatitis 6 weeks after the vaccination treatment (Fig 5, *A*), the MIF/TTX-vaccinated mice showed significant improvement (Fig 5, *B*). The clinical skin score of control-vaccinated mice increased after the vaccination, whereas that of MIF/TTX-vaccinated mice began to decrease at 21 weeks of age (Fig 5, *C*). At this time, the MIF/TTX-vaccinated mice showed high levels of anti-MIF antibodies (Fig 5, *D*). The serum IgE and MIF levels of MIF/TTX-vaccinated mice decreased at 21 weeks of age (Fig 5, *E* and *F*). These data show that MIF-DNA vaccination improves dermatitis not only in the DS-Nh strain but also in the NC/Nga mouse strains.

To confirm that anti-MIF antibodies suppress AD, we performed an additional therapeutic experiment by using a neutralizing anti-MIF mAb. Anti-MIF mAb (50 μg) or an isotypic control IgG (50 μg) were injected intravenously into 15-week-old NC/Nga mice with dermatitis twice a week for 3 weeks. Anti-MIF mAbs, as well MIF vaccination, significantly improved AD skin manifestations when compared with conditions seen in control IgG–treated mice (Fig 5, *G* and *H*).

Adoptive transfer of autoantibodies elicited by MIF/TTX-DNA vaccine suppressed AD

To better substantiate that the therapeutic action of MIF/TTX-DNA vaccination could be attributed to anti-MIF autoantibodies, we performed adoptive transfer of purified IgG from vaccinated DS-Nh mice into naive DS-Nh mice. The purified IgG was adoptively transferred into the 15-week-old DS-Nh mice that had already demonstrated skin eruptions. As shown in Fig 6, this IgG was effective in ameliorating AD, indicating that the therapeutic effect of MIF/TTX vaccination could be adoptively transferred by immune serum IgG.

DISCUSSION

In the present study we have shown that active vaccination against MIF is a novel preventive and therapeutic approach in 2 murine models of AD. We showed that mice administered a MIF/TTX-DNA vaccine did not experience the cutaneous manifestations of AD. The MIF/TTX-DNA vaccine also improved the symptoms

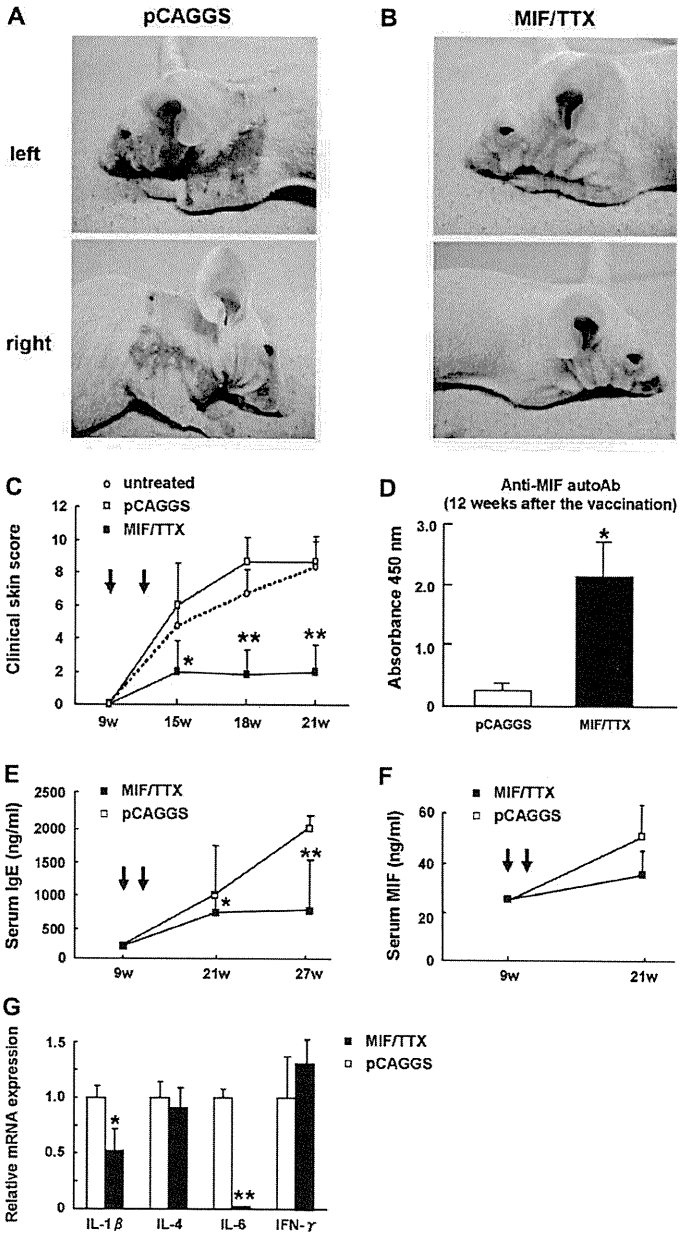

FIG 1. Prevention of the onset of AD by MIF/TTX-DNA vaccine. Nine-week-old DS-Nh mice without skin eruptions were subjected to administration of MIF/TTX or a control plasmid (pCAGGS). Clinical features of 21-week-old DS-Nh mice vaccinated with endotoxin-free pCAGGS **(A)** and MIF/TTX (**B**; 12 weeks after the vaccination) are shown. **C**, The clinical skin score of mice immunized with the MIF/TTX-DNA vaccine *(solid squares)*, immunized with pCAGGS plasmid *(open squares)*, or left untreated *(open circles)*. Results are given as means ± SEs of 5 mice in each group. $*P < .01$ and $**P < .005$ versus pCAGGS at the same time point. **D**, Serum level of anti-MIF autoantibodies *(autoAb)* at 12 weeks after vaccination. Means ± SEs are shown (n = 5). $*P < .01$. **E**, Serum IgE levels of the mice vaccinated with MIF/TTX *(solid squares)* and pCAGGS *(open squares)*. $*P < .01$ and $**P < .005$ for MIF/TTX versus pCAGGS at the same time point. Means ± SEs of 5 mice in each group are shown. **F**, Serum MIF levels of the mice vaccinated with MIF/TTX *(solid squares)* and pCAGGS *(open squares)*. **G**, Cytokine expression (IL-1β, IL-4, IL-6, and IFN-γ) in affected skin lesions was analyzed by using real-time PCR. $*P < .05$ and $**P < .001$.

of pre-existing AD in 2 different strains of AD-prone mice, the DS-Nh and NC/Nga strains. Finally, we demonstrated that the therapeutic effect of MIF/TTX vaccination could be adoptively transferred by serum IgG that contained MIF autoantibodies.

Proinflammatory cytokines are believed to be important contributors to the pathogenesis of skin inflammation in patients with AD, which might depend on the duration of the skin lesion. Patients with acute AD typically have a systemic T_H2 response

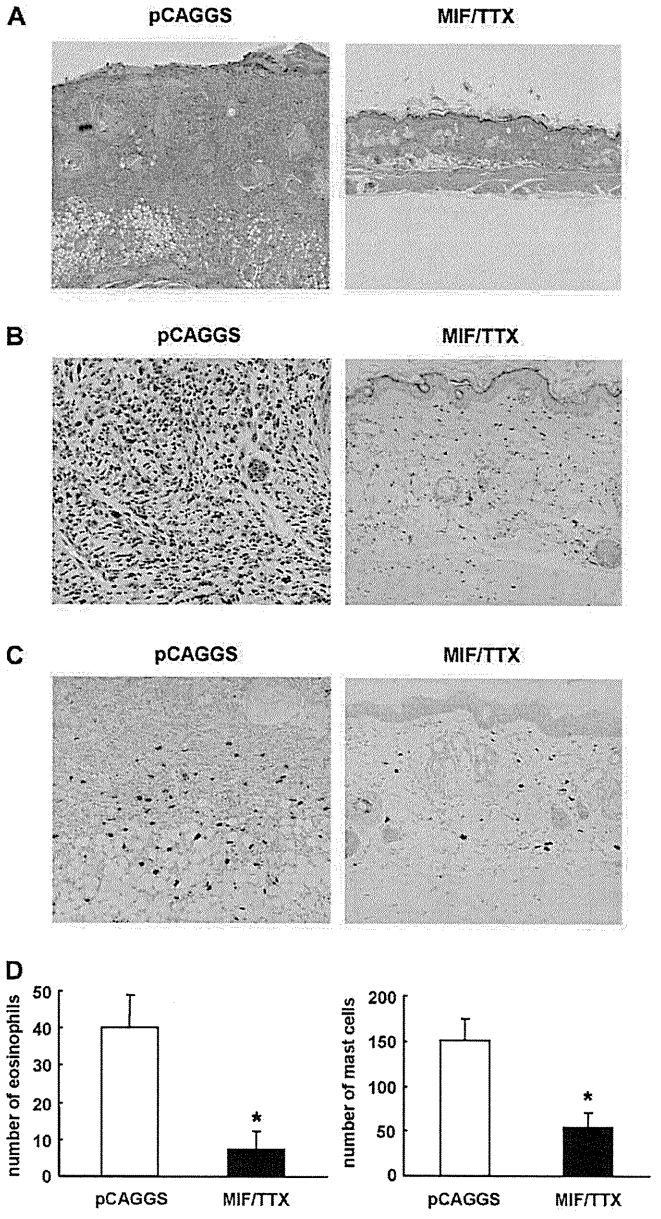

FIG 2. Histologic analysis of AD in DS-Nh mice vaccinated with MIF/TTX or pCAGGS plasmid before disease onset. Nine-week-old DS-Nh mice without eruptions were administered MIF/TTX or control plasmid. Specimens were collected from the dorsal skin 6 weeks after the first vaccination and stained with hematoxylin and eosin (**A**, original magnification ×40), direct fast scarlet for eosinophils (**B**, original magnification ×200), or toluidine blue for mast cells (**C**, original magnification ×200). **D**, The number of eosinophils and mast cells in 5 high-power fields from 4 individual skin specimens were enumerated by means of microscopy. Means ± SEs of 4 mice are shown. $*P < .001$ for MIF/TTX versus pCAGGS.

with increased serum IgE levels, eosinophilia, and a marked infiltration of T_H2 cells into acute skin lesions. The infiltrating T cells show a predominance of IL-4, IL-5, IL-10, and IL-13 expression.[12,18] In patients with chronic AD, however, there is infiltration of eosinophils and macrophages, and the disease becomes associated with an increase in the expression of IL-12, with a switch to T_H1 cellular responses.[12,18] Chronic AD skin lesions in adults with a prolonged duration of disease have been shown to manifest an increase in the expression of IL-1, IL-5, IL-12, IFN-γ, TNF-α, GM-CSF, and MIF.[12,18] This biphasic T_H1/T_H2 switch in immune response is characterized pathologically by lichenification, epidermal hyperplasia, and dermal fibrosis. MIF regulates the production of various proinflammatory cytokines, including TNF-α, and the inflammatory cytokines in response to stimulation by LPS are known to be suppressed in MIF-deficient mice. We previously reported that MIF-deficient mice have an impaired contact hypersensitivity (CH) response and that immunoneutralization of MIF effectively suppresses CH response[19]; these observations led us to speculate that MIF would be a therapeutic target for AD.

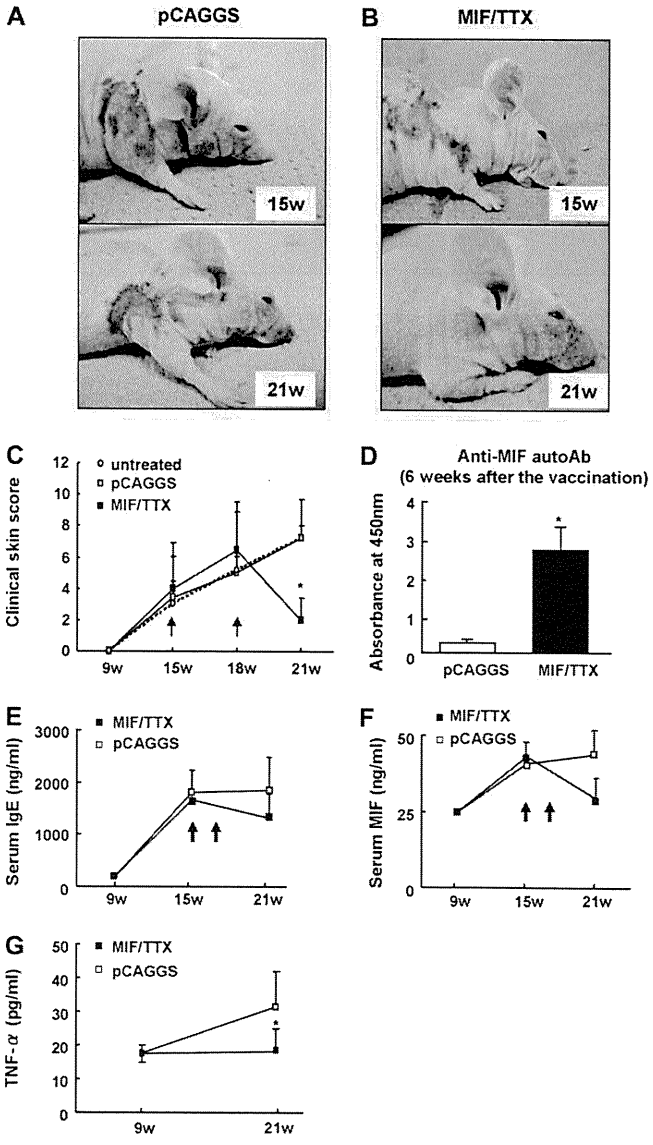

FIG 3. Therapeutic effect of MIF-DNA vaccination in DS-Nh mice with pre-existing AD. Fifteen-week-old DS-Nh mice with ongoing dermatitis were administered MIF/TTX or control plasmid (pCAGGS) or left untreated. **A**, Clinical features of DS-Nh mice vaccinated with control plasmid. **B**, Clinical features of DS-Nh mice vaccinated with MIF/TTX. **C**, Clinical skin scores of mice immunized with MIF/TTX-DNA vaccine *(solid squares)*, control plasmid *(open squares)*, or left untreated *(open circles)*. Means ± SEs of 10 mice per group are shown. $*P < .005$ for MIF/TTX versus pCAGGS. **D**, Serum level of anti-MIF autoantibodies *(autoAb)* at 6 weeks after the vaccination. Means ± SEs are shown (n = 10). $*P < .001$. Serum IgE **(E)** and MIF **(F)** levels of the mice vaccinated with MIF/TTX vaccine *(solid squares)* and control pCAGGS plasmid *(open squares)* are shown. The data shown are for 10 mice per group. **G**, The serum levels of TNF-α were decreased in MIF/TTX-vaccinated mice *(solid squares)* compared with those seen in the control (pCAGGS) plasmid–vaccinated mice *(open squares)*. $*P < .01$ for MIF/TTX versus pCAGGS.

The therapeutic aim of cytokine vaccine therapy is to induce high titers of circulating polyclonal autoantibodies to neutralize the pathologic levels of a particular cytokine. The advantages of this therapy include the potential to maintain high antibody titers, long-term efficacy, and low cost. Monoclonal antibodies directed against TNF-α have been used for the treatment of psoriasis.[10] Jacobi et al[7] recently reported a clinical trial of infliximab monotherapy for 9 patients with moderate or severe AD who showed significant improvement in all clinical parameters; however, this improvement was not sustained by maintenance of the therapy. The authors considered that the development of antichimeric antibodies could explain the lack of a durable response to infliximab maintenance therapy. A cytokine vaccine results in the production of native antibodies, and it might overcome this limitation in anti-cytokine antibody therapy.

It is unknown whether long-term inhibition of MIF activity might be safe in human subjects. A major limitation of an active immunization approach is the inability to control the outcome. However, it should be noted that serum MIF levels in the MIF-DNA–vaccinated mice were maintained at a baseline level

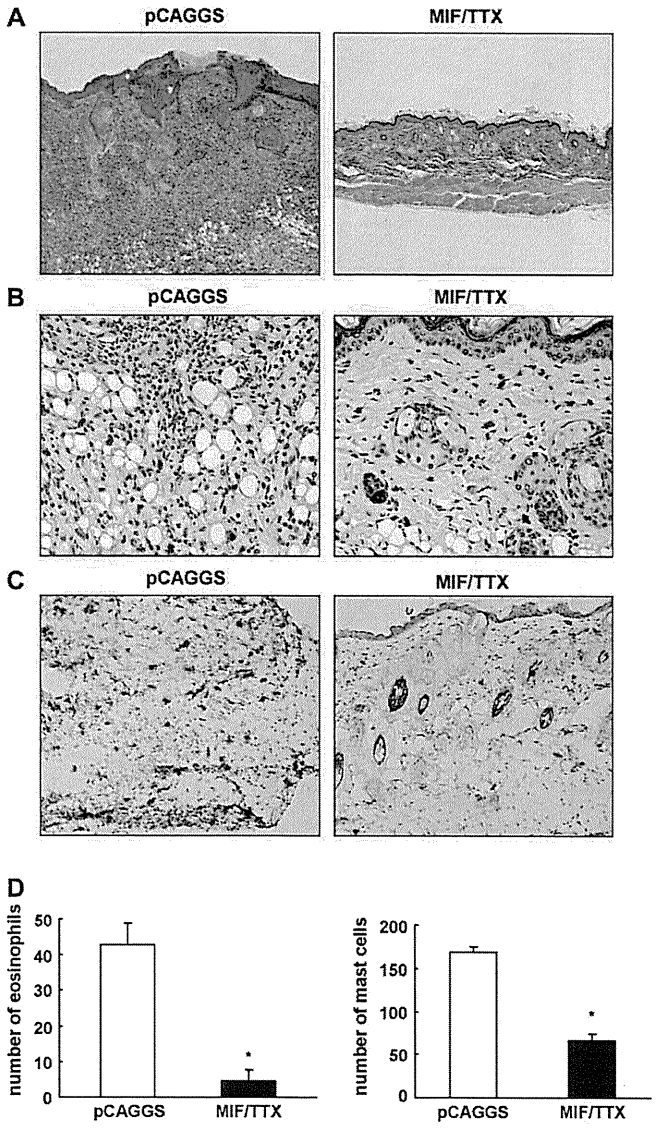

FIG 4. Histologic analysis of AD in DS-Nh mice vaccinated with MIF/TTX or control plasmid after disease onset. Fifteen-week-old DS-Nh mice with ongoing dermatitis were administered MIF/TTX or control (pCAGGS) plasmid. Specimens were collected at 6 weeks after the first vaccination and stained with hematoxylin and eosin (**A**, original magnification ×40), direct fast scarlet for eosinophils (**B**, original magnification ×200), or toluidine blue for mast cells (**C**, original magnification ×200). **D**, The number of eosinophils and mast cells in 5 high-power fields from 4 individual skin specimens were enumerated by means of microscopy. Data represent means ± SEs of 4 mice. $*P < .001$ for MIF/TTX versus pCAGGS.

(Figs 2, *F*, and 4, *F*), despite an anti-MIF antibody level that remained high for 6 weeks of vaccine administration. It is possible that the present protocol of vaccination dose not induce a high enough level of anti-MIF antibody to inhibit serum MIF protein completely. There are reports that autoantibody production induced by vaccine-encoded antigens regress to baseline levels shortly after remission in acute experimental autoimmune encephalomyelitis,[15] whereas in adjuvant-induced arthritis[16] autoantibodies continue to be produced at high titer. It has been considered that targeted DNA vaccines amplify a pre-existing anti–self-regulatory response that by itself is capable of limiting, although not preventing, the emerging autoimmune condition.[15-17,20-22] In addition, we observed that MIF-DNA–vaccinated mice did not show serious side effects, such as evident infections.

Serum IgE levels were significantly decreased when MIF vaccination was used as a preventive agent, whereas the levels were not significantly decreased when it was used as a therapeutic agent. It is known, however, that IgE levels do not parallel the clinical severity of AD in human patients.[19]

The cardinal principles in the treatment of AD are to reduce symptoms, prevent exacerbations, and minimize medication side effects. This approach incorporates the use of emollients, topical corticosteroids, topical calcineurin inhibitors, antihistamines, stress management, and avoidance of allergens or